

Growing length scales in aging systems

Federico Corberi

*Dipartimento di Matematica ed Informatica, Università di Salerno, via Ponte don Melillo,
84084 Fisciano (SA), Italy*

Leticia F. Cugliandolo

*Université Pierre et Marie Curie - Paris VI, Laboratoire de Physique Théorique et Hautes
Energies, 4 Place Jussieu, Tour 13, 5ème étage, 75252 Paris Cedex 05, France.*

Hajime Yoshino

*Department of Earth and Space Science, Faculty of Science, Osaka University, Toyonaka
560-0043, Japan.*

OXFORD
UNIVERSITY PRESS

Abstract

We summarize studies of growing lengths in different aging systems. The article is structured as follows. We recall the definition of a number of observables, typically correlations and susceptibilities, that give access to dynamic and static correlation lengths. We use a growing length perspective to review three out of equilibrium cases: domain growth phenomena; the evolution of Edwards-Wilkinson and Kardar-Parisi-Zhang manifolds and other directed elastic manifolds in random media; spin and structural glasses in relaxation and under an external drive. Finally, we briefly report on a mechanism for dynamic fluctuations in aging systems that is based on a time-reparametrization invariance scenario and may be at the origin of the dynamic growing length in glassy materials.

1 Introduction

For a long time, and somewhat paradoxically, the majority of theoretical physicists interested in glasses were reluctant to study these systems in the truly glassy regime, say below the glass temperature T_g or above the glass density ρ_g . One of the reasons to resist entering the glassy regime was the lack of insight on which questions to ask and, more concretely, which quantities to measure in out of equilibrium conditions.

The situation changed dramatically around 20 years ago when it was accepted that glassy systems do not freeze out below T_g but they just continue to relax at a slower and slower rate as time goes by – the *aging* phenomenon. Although this fact was well-known experimentally and to a certain extent also numerically it was not fully assimilated theoretically. The solution to a number of simple models [namely, droplet models for disordered systems (1), random walks among traps in phase space (2), and mean-field spin systems with disordered interactions (3; 4)] demonstrated the possibility of capturing aging phenomena analytically. These solutions also provided a guideline as to which are the simplest preparation protocol and the most relevant observables to focus on dynamically. More importantly, these studies also opened the way to confront glassy dynamics to the behaviour of other macroscopic non-equilibrium systems considered to be simpler such as coarsening phenomena (5) or the motion of manifolds in different kinds of embedding volumes (6). Experimental and numerical data on theoretically motivated measurements in various physical systems have rapidly accumulated and some of these results are summarized in other chapters in this book.

As for the measuring protocols, in short, one first chooses the way in which the system is taken into the glassy regime and defines the origin of the time axis accordingly. In the simplest setting, the ‘initial time’ $t = 0$, is the instant when the system is suddenly prepared in an out-of-equilibrium condition. For instance, this is achieved by performing a rapid temperature quench from a high temperature above T_g down to a target value $T < T_g$ but other routes to the glassy regime, changing other control parameters, are also feasible. As will be discussed below, the physical properties of the system become functions of the waiting time t_w , the time spent after the preparation of the initial state, stationarity is lost and the relaxation time increases with t_w . The basic idea to analyze such an aging relaxation is to introduce a laboratory time scale – the waiting-time – that can be controlled at will when the intrinsic time scale – the equilibrium relaxation time – goes beyond accessible times.

Following this procedure one can study, for instance, the energy relaxation as a function of t_w . However, such a macroscopic ‘one-time quantity’ does not capture all the richness of the relaxation. Much more detailed information is contained in two (or more) time-dependent global quantities. In Fig. 1.1 we show the typical behaviour of two *macroscopic* two-time quantities in many glassy systems: the spontaneous decorrelation of a chosen global observable measured at two subsequent times t and t_w

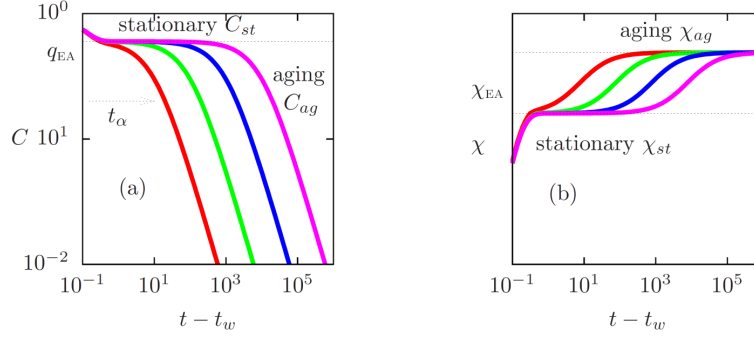


Fig. 1.1 Typical behaviour of macroscopic two-time quantities during aging. (a) Auto-correlation function $C(t, t_w)$; (b) linear-susceptibility $\chi(t, t_w)$. The waiting time t_w increases from the left to the right curves, typically in a logarithmic scale such that, say, $t_{w,k+1} = 10t_{w,k}$. The α relaxation time, t_α , or the time-difference needed to decorrelate significantly, is an increasing function of t_w and is indicated with an arrow in the left panel. The plateau in χ occurs at $\chi_{ea} = (1 - q_{ea})/T$ where q_{ea} is the height of the plateau in C .

(a), and the linear response of the same observable measured at t to a perturbation that couples linearly to it between t_w and t (b).

As shown in panel (a), the auto-correlation function exhibits a two-step decay. At short time scales, say $t - t_w \ll t_w$, there is a relaxation towards a plateau that we call the Edwards-Anderson (EA) order-parameter q_{ea} (see its precise definition in Eq. (6)). The relaxation in this stage is essentially independent of the waiting time t_w and time-translational invariance (TTI) holds $C(t, t_w) = C_{st}(t - t_w)$ to a certain accuracy. The second relaxation at longer time scales, say $t - t_w \gg t_w$, exhibits t_w -dependence and is not stationary. The latter reflects the strong out-of-equilibrium nature of aging. The separation of time-scales is confirmed in panel (b) where we sketch the behaviour of the susceptibility $\chi(t, t_w)$. The plateau occurs here at $\chi_{ea} = (1 - q_{ea})/T$ with q_{ea} the value of C at its plateau and T the temperature of the environment that is henceforth measured in units of k_B , the Boltzmann constant.

The relaxation of the correlation in Fig. 1.1 (a) reminds us, in a sense, of the two step relaxation in the supercooled liquid phase – the so-called α and β relaxations (7). Even more so, it is basically indistinguishable from the one found in phase ordering processes after a temperature quench (see Sect. 3 for a detailed description of coarsening) (5). In such processes domains of the different equilibrium phases progressively grow in competition. At each instant, the equilibrium order parameter is essentially uniform within each domain. When only short time-differences are explored the domain-walls are basically static and the correlations decay just as in equilibrium.

Instead, when longer time-differences are reached the walls move appreciably and the correlations decay from the plateau in a manner that depends explicitly on the waiting-time. A key quantity in the description of coarsening is the *typical domain linear size*, $L(t)$, which plays the role of a dictionary between time t and length L . All properties of coarsening systems are invariant under rescaling of all lengths by $L(t)$ – in a statistical sense.

The question naturally arises as to whether the dynamics in glassy systems is also of coarsening type albeit the growing order had not been identified yet. From the analysis of the correlations in many glasses, and one example is shown in Fig. 1.2 where scaled data from an aging colloidal suspension are displayed (8), one could easily conclude this to be the case. The figure shows the two-time correlation data taken using different t_w s as a function of the ratio t/t_w . For sufficiently long t_w the scaling is quite good suggesting that there might be a growing length $L(t) \propto t^a$, with a an undetermined power. However, the scaling of the global two-time correlation as $f(L(t)/L(t_w))$ is just a quite generic property of two-time correlations (4), and the space-time correlations do not signal the growth of structure contrary to what happens in simple phase ordering kinetics in which it scales as a function of $r/L(t)$. Therefore, to reach a conclusion on the existence (or not) of a growing length one should, ideally, analyze the dynamics at *mesoscopic time and length scales* or, at least, define and explore more complex quantities giving access to the mesoscopic details of the process. Eventually, these studies might also enlighten us about the reason for the growth.

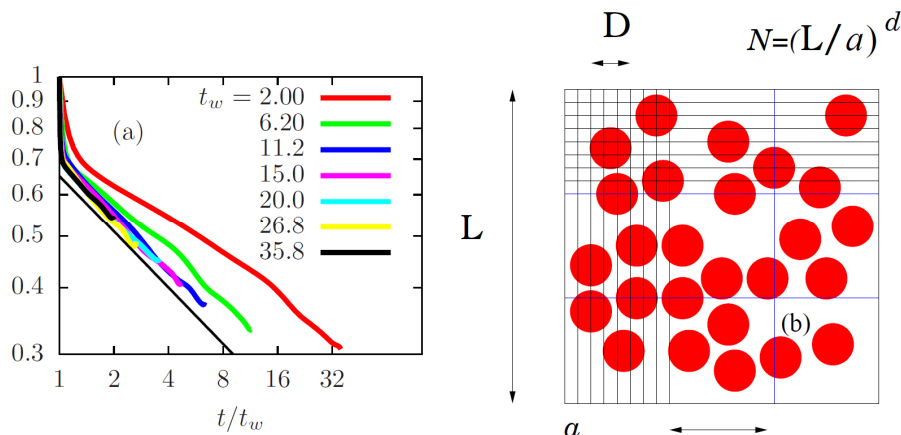


Fig. 1.2 (a) Scaling of two-time correlation data in an aging colloidal suspensions. Waiting times are given in the key in units of 10^2 s. The relatively good scaling with t/t_w suggests $L(t) \simeq t^a$. The data are taken from and analyzed along the lines explained in (8). (b) A sketch of the pixelization used to describe the particle configurations with binary variables, $\sigma_\alpha = 0, 1$; and the coarse-graining procedure (see Sec. 2.1). a is the lattice spacing, D the particle diameter, ℓ the coarse-graining length and L the system size.

Taking the case of usual phase ordering processes as a reference, we realize that in order to settle this issue we need to follow a number of basic steps summarized by the following questions: 1) how can we define an order parameter for a glass? 2) how can we define domains – within which the order parameter is essentially constant – or dynamically correlated volumes? 3) can one identify a growing linear size and does it reflect the nature of the dynamics - e.g. smooth (such as, for instance, the curvature driven kinetics observed in some coarsening systems) vs. activated? 4) can one understand the mechanism leading to such a growth? In the body of this chapter we develop these questions.

Having explained that the aim of this chapter is to discuss searches of growing lengths in *aging glasses*, we announce that we shall also deal with *a priori* simpler cases such as a particle's diffusion in random media or the motion of a finite dimensional manifold, both in their aging regime. Although the glassy nature of these problems might not be complete, it turns out that some aspects of their dynamics are similar to the ones encountered in conventional glasses. Moreover, their mere definition is clearer and their analytic treatment as well as the identification of a growing length are simpler. Their discussion should then be instructive.

The organization of the chapter is the following. In Sect. 2 we give a number of definitions and we discuss how to deal with quenched disorder, if present. In Sect. 3 we review sub-critical and critical coarsening phenomena in clean systems. In this Section we also introduce, briefly, a relatively simpler problem with an easy to identify growing length: the motion of a free elastic manifold. Section 4 is devoted to the phenomenological description of activated processes – that are specially relevant in problems with quenched disorder – starting with a short account of aging in the Sinai model of diffusion and developing afterwards the droplet model predictions for the dynamics of elastic manifolds in random media and spin-glasses. Section 5 recaps mean-field predictions for the growing length issued from the study of fully-connected spin models and the related mode-coupling theories as well as growth phenomena in kinetically constrained models for glasses. We also discuss growing lengths in other systems with aging dynamics: the interplay between flow and internal relaxation and the effect of the former on the aging properties of coarsening and glassy systems, granular matter and quantum glasses. Finally, in Sect. 6 we briefly recall a possible mechanism for dynamic fluctuations and the associated growing correlation length in aging systems: the asymptotic development of time-reparametrization invariance, that has been extensively reviewed elsewhere (9).

We do not attempt to present a comprehensive review of analytic, numeric and experimental studies of all kinds of aging systems. We rather focus on the search for growing length-scales and their possible use to describe aging materials. With this in mind, the reader should not expect to find a complete list of references on aging studies.

2 Definitions

In this Section we summarize a number of definitions relevant to the study of cooperative motion in glassy systems. These definitions do not assume equilibrium and can be used to study out of equilibrium and, in particular, aging samples. They depend,

in general, on various times independently and no fluctuation-dissipation theorem is assumed. Although we are not going to dwell into the question of the pertinence of effective temperatures in the description of glasses, we recall its definition since it will appear in the rest of this Chapter.

2.1 Euler and Lagrange descriptions

Two ways of studying the heterogeneous dynamics in a many particle (or many higher-dimensional object) system are the following.

Lagrangian description. One can follow the evolution of each individual particle, labeled by an index i , and detect which are the fast and slow moving ones during a previously chosen time window, say $t - t_w$, around some time, say t_w , after preparation. This is the route followed in early studies of dynamic heterogeneities in supercooled liquids, see (10) and (11) for a few of many molecular dynamics and confocal microscopy papers that use this type of measurement. One of the main outcomes of these studies is the observation of clustering of fast particles, in the form of strings the length of which increases – and may diverge – close to the glassy arrest. In the trully glassy phase fewer studies exist. A precursor is (12). More recently, Vollmayr-Lee *et al* studied the geometry and statistical properties of clusters of mobile and immobile particles with molecular dynamics (13). Confocal microscopy has been used with similar aims (14).

Eulerian description. In a first step, one can define Ising spin variables as the ones that describe uniaxial magnetic systems. The choice is done for notation convenience but also because, as proposed in (8), a simple mapping between particle positions and Ising spin variables, σ_α , defined on the $N = (L/a)^3$ vertices of a cubic lattice captures the dynamics of ‘atomic’ glassy systems as well (see Fig. 1.2-(b)). (L is the linear length of the box and a the length of the lattice spacing.) In a few words, one partitions space with a lattice with very fine mesh – smaller than the particle radii – and the mapping assigns a spin one to each cell occupied by a piece of particle and zero otherwise. Once this is done, all observables are written in terms of the bimodal variables, as in spin models, and the identities of the particles are ignored.

In a second step, one can coarse-grain the spin variables over boxes of a chosen linear size, ℓ , with ideally $L \gg \ell \gg a$. The locality is then given by the position of the box which is labeled by an index i . The coarse-graining amounts to a partial averaging, the effective spin on each box, s_i , is now a continuous variable, $0 \leq s_i \leq 1$.

In a system with quenched randomness, realized as fixed obstacles, local fields or else, the coarse-graining procedure over a sufficiently large volume averages over the peculiar local features of the fixed disorder. In this way, the ‘finger-print’ (15) of disorder, that is to say local fluctuations determined by the particular local disorder – such as Griffiths singularities in random ferromagnets – should be washed away. One can then expect to arrive at a description of the noise-induced fluctuations present in problems with or without quenched disorder.

This method appears to be more adequate for analytic treatment through a field theory.

2.2 Space-time correlation

In usual coarsening systems, see Sect. 3, the averaged space-time correlation function

$$NC(r, t) = \sum_{ij/|\vec{r}_i - \vec{r}_j| = r} \langle \delta s_i(t) \delta s_j(t) \rangle, \quad (1)$$

with $\delta s_i(t) = s_i(t) - \langle s_i(t) \rangle$ and $\langle s_i(t) \rangle = \langle s_i \rangle_{eq}$ in all the cases we shall deal with, allows for the identification of a growing length from, for example, $L_a(t) \equiv \int d^d r r^{a+1} C(r, t) / \int d^d r r^a C(r, t)$. (a is a parameter chosen to weight preferentially short or long distances; the time-dependence of $L_a(t)$ should not depend on a.) Here and in the following $\langle \dots \rangle$ stands for an average over different realizations of thermal histories at heat-bath temperature T and/or initial conditions. In presence of quenched disorder one adds an average over it and denotes it $[\dots]$. The stochastic time-dependent function $N^{-1} \sum_{ij/|\vec{r}_i - \vec{r}_j| = r} s_i(t) s_j(t)$ after a quench from a random initial condition does not fluctuate in the thermodynamic limit. Therefore, the averages are not really necessary but they are usually written down. In spin-glasses and glasses this observable does not yield information on the existence of any growing length as we shall discuss below.

2.3 Two-time quantities

The auto-correlation function and linear susceptibility are defined as

$$\begin{aligned} NC(t, t_w) &\equiv \sum_{i=1}^N \langle C_i(t, t_w) \rangle = \sum_{i=1}^N \langle \delta s_i(t) \delta s_i(t_w) \rangle, \\ N\chi(t, t_w) &\equiv \sum_{i=1}^N \langle \chi_i(t, t_w) \rangle = \sum_{i=1}^N \int_{t_w}^t dt' R(t, t'), \end{aligned} \quad (2)$$

with $R_i(t, t') = \delta \langle s_i(t) \rangle / \delta h_i(t')|_{h=0}$ and $NR = \sum_{i=1}^N R_i$ the local and global instantaneous linear responses, respectively.

A number of fully general relations between the linear response and a correlation computed as an average over unperturbed system trajectories have been recently derived. Quite generally they read

$$R(t, t_w) = \frac{1}{2T} \left[\frac{\partial C(t, t_w)}{\partial t_w} + N^{-1} \sum_{i=1}^N \langle s_i(t) B_i(t_w) \rangle \right] \theta(t - t_w). \quad (3)$$

The explicit form of the factor B_i in the second term in the right-hand-side (r.h.s.) depends on the microscopic dynamics; it has been computed for Langevin processes (16) and Markov processes for discrete variables (17). In all cases B_i is the deterministic drift in the sense that $\langle \dot{s}_i \rangle = \langle B_i \rangle$.

In equilibrium, the second term in the r.h.s. of Eq. (3) is equal to the first one, and R (or χ) and C are related by the fluctuation-dissipation theorem

$$R(t, t_w) = \frac{1}{T} \frac{\partial C(t, t_w)}{\partial t_w} \theta(t - t_w), \quad (4)$$

$$\chi(t, t_w) = \frac{1}{T} [C(t, t) - C(t, t_w)] \theta(t - t_w), \quad (5)$$

and all two-time quantities depend on $t - t_w$ only.

2.4 Order parameter

The very concept of a glass order parameter is not obvious. Although some kind of static amorphous order may develop with time in a glassy regime, searches have given negative results so far (not surprisingly since one does not really know what is looking for) (18). The simplest possibility, $\langle s_i(t) \rangle$, is void of information and the space-time spin-spin correlation $C(r, t)$ (the Fourier transform of the structure factor) is, to a first approximation, time independent and very similar to the one in the super-cooled liquid (8).

Edwards-Anderson order parameter. A *dynamic* order parameter, named after Edwards and Anderson (EA) who introduced it for spin-glasses, is defined as

$$q_{ea} = \lim_{t \rightarrow \infty} \lim_{t_w \rightarrow \infty} C(t, t_w) , \quad (6)$$

where $C(t, t_w)$ is the auto-correlation function. The order of the two long time limits is crucial since the weak long-term memory (2; 3) ensures that $\lim_{t_w \rightarrow \infty} \lim_{t \rightarrow \infty} C(t, t_w) = 0$ (see Fig. 1.1 (a)). The EA order parameter detects ergodicity breaking: in the liquid (paramagnetic) phase $q_{ea} = 0$ because the system loses memory at finite time scales but in the glass phase such memory remains. The idea is quite generic and it can be applied to glassy systems made of constituents of any kind.

Replica overlap - a static counterpart. The theory of spin-glasses (19) suggests the definition of a *static* order parameter as the *overlap* between two replicas (two systems with the same quenched randomness) a and b subjected to a fictitious attractive coupling of strength ϵ that forces them to be in the same thermodynamic state:

$$q = \lim_{\epsilon \rightarrow 0} \lim_{N \rightarrow \infty} \frac{1}{N} \sum_{i=1}^N \langle s_i^a s_i^b \rangle_{\epsilon} . \quad (7)$$

The *spin-glass susceptibility* is its linear response to an infinitesimal variation of the coupling:

$$\chi_{sg} = \left. \frac{\partial q}{\partial \epsilon} \right|_{\epsilon=0} = \frac{\beta}{N} \sum_{i,j} \left(\langle s_i^a s_j^a s_i^b s_j^b \rangle - \langle s_i^a s_j^a \rangle \langle s_i^b s_j^b \rangle \right) . \quad (8)$$

The averages $\langle \dots \rangle_{\epsilon}$ and $\langle \dots \rangle$ are taken here with the corresponding Gibbs-Boltzmann distributions. A crucial problem with these definitions is that below T_g aging persists at any finite (with respect to some function of N) time scale. Nonetheless, χ_{sg} motivates the definition of a dynamic analogue that could detect the growth of static order during aging, see Sect. 2.6.

2.5 Dynamically correlated volume

A more natural proposal is to consider the spatial variation of the *speed of relaxation* in different regions of space. This point of view is very close in spirit to the idea of dynamical heterogeneity in the supercooled liquid regime as characterized by local relaxation times. As discussed later, this point of view also emerges naturally in the

theoretical analysis of soft-modes associated with the time reparametrization invariance in the effective dynamical equations of motion at long time scales (9). We present below different ways to access a correlation related to the local dynamics.

Spatial correlation of local dynamics. Let us regard the local two-time dependent auto-correlation function $C_i(t, t_w)$ as the *local order parameter*. Its spatial variation can be easily characterized by the spatial correlation function (15; 20; 21)

$$G_4(i, j; t, t_w) = \langle C_i(t, t_w) C_j(t, t_w) \rangle - [C(t, t_w)]^2. \quad (9)$$

The subscript 4 is to remind one that it is a 4-point function since the auto-correlation function is already a two-point correlation function (in time).

The key question is whether there is a characteristic dynamical length-scale, $\xi_4(t, t_w)$, beyond which G_4 de-correlates, e.g.

$$-\ln G_4(i, j; t, t_w) \simeq \frac{r}{\xi_4(t, t_w)} + b \ln r \quad (10)$$

with $r = |\vec{r}_i - \vec{r}_j|$. [This expression assumes the usual decay $G_4 \sim r^{-b} \exp(-r/\xi_4)$ but more general forms of the type $G_4 \simeq r^{-b} f(r/\xi_4)$ have also been considered.]

By integrating Eq. (10) over space one obtains

$$N\chi_4(t, t_w) = \sum_{i,j} G_4(i, j; t, t_w) = \langle [\sum_i C_i(t, t_w)]^2 \rangle - \langle \sum_i C_i(t, t_w) \rangle^2 \quad (11)$$

which measures the dynamically correlated volume. Note that in spite of being usually called a ‘susceptibility’, strictly speaking χ_4 is not one (22; 23). The same proviso applies to χ_{sg} in Eq. (13).

The 4-point correlation function in Eq. (9) and the integrated one in Eq. (11) are extensions of similar expressions defined for the supercooled (stationary) liquid state. In the glassy regime one needs to keep the t_w dependence in $\xi_4(t, t_w)$. Still, it can be measured in numerical simulations and in some experiments from real-time real-space images. One has to keep in mind, though, that this quantity detects how similar motion in different regions is but not necessarily whether these are ordering in the same state.

Higher order susceptibilities. Although G_4 has been studied in numerical simulations (21; 24) its direct experimental investigation remains a challenge as, in general, multi-point correlators. (Lucky exceptions are colloidal suspensions in which confocal microscopy allows one to store the full particle configuration (8).) A natural way out would be to measure responses to external perturbations, actual susceptibilities, as suggested in (25; 26) and done experimentally in (27). The basic idea is that G_4 should be related to a non-linear susceptibility by some sort of generalization of the FDT, much in the same way as the ordinary correlation function is linked to the linear susceptibility, see Eq. (5). One could then measure the latter to extract information on the former. In order to fulfill this program it is necessary to establish which are the non-linear susceptibilities associated to multi-point correlators and which is the generalization of the FDT, holding possibly out of equilibrium. Exact general relations

between multi-point correlators and non-linear response functions (22; 23; 26) derived for systems subjected to a Markovian dynamics show that beyond linear order the susceptibilities are related not only to multi-spin correlations (such as G_4) but also to more complicated correlators. For instance, for the second order response of two spins $R_{ij}^{(2)}(t, t_1, t_2) = \delta^2 \langle s_i(t) s_j(t) \rangle / \delta h_i(t_1) \delta h_j(t_2) |_{h=0}$ in equilibrium one has

$$R_{ij}^{(2)}(t, t_1, t_2) = \frac{1}{2T} \left[\frac{\partial}{\partial t_1} \frac{\partial}{\partial t_2} \langle s_i(t) s_j(t) s_i(t_1) s_j(t_2) \rangle - \frac{\partial}{\partial t_2} \langle s_i(t) s_j(t) B_i(t_1) s_j(t_2) \rangle \right], \quad (12)$$

for $t_1 \neq t_2$. This feature poses the problem of choosing the best suited non-linear susceptibility to detect cooperative effects. In a series of papers both third (26) and second (23) order susceptibilities have been considered. Analytical and numerical studies show that the non-linear susceptibilities and G_4 obey analogous scaling forms from which one can extract a cooperative length. Experimental studies are on the way (28).

The second order susceptibility $\chi^{(2)}(t, t_w) = \int_{t_w}^t dt_1 \int_{t_w}^t dt_2 R_{ij}^{(2)}(t, t_1, t_2)$ is strictly related to the fluctuations of $\chi_i(t, t_w)$ (23; 29).

Distributions of coarse-grained two-time quantities. Another way of extracting a growing length, ξ , alternative to that expressed by Eq. (10), is to study the full distribution of local two-time functions (15; 30; 31; 32). Indeed, for $\ell \gg \xi$ the coarse-graining boxes naturally become independent and one should recover a Gaussian distribution. The crossover from non-trivial to trivial dependence can then be used to estimate ξ that should, presumably, behave as ξ_4 . The same argument can be applied to the pdf of the local linear susceptibility χ_i s.

2.6 Growth of underlying static glass order?

An intriguing problem is whether any static glass order develops during aging. The spin-glass susceptibility, Eq. (8), suggests to define a 4-point correlation function (24; 25; 33; 34; 35; 36),

$$N\chi_{sg}(t) = \sum_{i,j} G_{sg}(i, j; t) = \sum_{i,j} \langle s_i^a(t) s_j^a(t) s_i^b(t) s_j^b(t) \rangle. \quad (13)$$

Time t is measured after the temperature quench at which the two replicas, labeled a and b , are prepared in independent random initial configurations. One is interested in finding a dynamic length-scale, $\xi_{sg}(t)$, beyond which G_{sg} decorrelates,

$$-\ln G_{sg}(i, j; t) \sim \frac{r}{\xi_{sg}(t)} + c \ln r. \quad (14)$$

$\xi_{sg}(t)$ is simpler than $\xi_4(t, t_w)$ in that it is a one-time quantity like the domain size $L(t)$ in usual phase ordering processes.

In the context of spin-glasses the value of the parameter c is used to distinguish between a disguised ferromagnet picture, as proposed in the droplet model (1),

and a more complex equilibrium structure, such as the one predicted by mean-field models (19). In the former $\lim_{r \rightarrow \infty} G_{sg}(r) \rightarrow \text{const}$ and $c = 0$ while in the latter $\lim_{r \rightarrow \infty} G_{sg}(r) \rightarrow 0$ and $c > 0$.

It is interesting to compare $\chi_{sg}(t)$ and $\chi_4(t, t_w)$. Since there are no interactions between the two replicas a and b , purely dynamic correlation cannot exist between them. Thus, the dynamical SG susceptibility $\chi_{sg}(t)$ can only detect growth of (if any) static order much as domains in usual phase ordering. On the other hand $\chi_4(t, t_w)$ can detect both static and dynamic order.

2.7 Effective temperature

Although we shall not develop the T_{eff} ideas here we include a short paragraph recalling its definition; the concept will appear in a number of places later in the article.

The deviation from the fluctuation-dissipation theorem (FDT) found in mean-field glassy models (3; 4) and in a number of finite dimensional systems (37) can be rationalized in terms of the generation of an effective temperature (38) in the system. The identification of a temperature out of equilibrium makes sense in the asymptotic limit of small entropy production (either long times or very weak applied drive, see Sec. 5.4) in which the system evolves slowly. T_{eff} is defined as minus the inverse slope of the asymptotic parametric plot $\chi(C)$, where χ is the linear integrated response and C is the two-time correlation. The thermodynamic character of T_{eff} has been checked in mean-field models and mode-coupling theories as well as in simulations of Lennard-Jones mixtures, models of silica and many others. A basic condition is that T_{eff} obtained from different (interacting) observables should be equal whenever measured in the same dynamic regime. A different scenario is found at the lower critical dimension and in critical dynamics, and in trap models with unbounded trap depths.

3 Phase ordering

Phase-ordering kinetics is an important problem for material science but also for our generic understanding of pattern formation in nonequilibrium systems.

Let us consider a physical macroscopic system in contact with an external reservoir in equilibrium. Imagine now that one changes a parameter instantaneously in such a way that the system is taken from a disordered phase to an ordered one in its (equilibrium) phase diagram. Two paradigmatic examples are spinodal decomposition, *i.e.* the process whereby a mixture of two or more substances separate into distinct regions with different concentrations, and magnetic domain growth in ferromagnetic materials quenched below the Curie temperature (5).

Closely related to the above is the process whereby a critical state is approached via a quench from the disorder state right to the temperature at which the phase transition occurs.

In both sub-critical and critical coarsening the dynamical process starts from an equilibrium high temperature disordered state and progressively evolves building a new phase, stable at a lower temperature, either ordered or critical.

3.1 Growing length, aging and scaling

The evolution of an initial condition that is not correlated with the final equilibrium state (and with no bias fields) does not reach equilibrium in finite times. More explicitly, domains of all the phases of the equilibrium state at the final temperature T keep on growing, until their typical size $L(t)$ becomes of the order of the system size L . For any shorter time the system is out of equilibrium and, in particular, the non-equilibrium evolution does not come to an end whenever the thermodynamic limit $L \rightarrow \infty$ is taken at the outset.

The very existence of a growing length $L(t)$ is at the heart of the aging behavior observed in these systems as can be easily understood. Since $L(t_w)$ increases with t_w the system needs larger rearrangements to decorrelate from older configurations. This simple fact is the origin of the strong t_w -dependence of the autocorrelation and linear-response described in Sec. 1 and depicted in Fig. 1.1.

In the asymptotic time domain, when $L(t)$ has grown much larger than any microscopic length in the system, a *dynamic scaling* symmetry sets in, similarly to the usual scaling symmetry observed in equilibrium critical phenomena. According to this hypothesis, the growth of $L(t)$ is the only relevant process and the whole time-dependence enters only through $L(t)$. Observables such as correlation and response functions take precise scaling forms that will be discussed in Secs. 3.2 and 3.3. Exceptional cases where dynamic scaling is not observed will be shortly discussed in Sec. 3.3.

3.2 Aging at a critical point

The scaling behavior of binary systems quenched to the critical point is quite well understood since this issue can be addressed via scaling arguments (39) and renormalization group approaches (40) which give explicit expressions for many of the quantities of interest up to two loops order. Numerical simulations (41) confirm the analytic results and probe exponents and scaling functions beyond the available perturbative orders. In this case the system builds correlated critical clusters with fractal dimension $D = (d + 2 - \eta)/2$, where η is the usual static critical exponent, in regions growing algebraically as $L(t) \sim t^{1/z_{eq}}$, z_{eq} being the dynamic equilibrium critical exponent relating times and lengths.

In the asymptotic time domain the correlation function (1) has the scaling form

$$C(r, t) = L(t)^{-2(d-D)} f\left(\frac{r}{L(t)}\right). \quad (15)$$

The pre-factor $L(t)^{-2(d-D)}$ takes into account that the growing domains have a fractal nature (hence their *density* decreases as their size grows) and the dependence on $r/L(t)$ in $f(x)$ expresses the similarity of configurations at different times once lengths are measured in units of $L(t)$.

For two-time quantities, when t_w is sufficiently large one has

$$C(t, t_w) = C_{st}(\tau) f_c\left(\frac{L(t)}{L(t_w)}\right), \quad R(t, t_w) = R_{st}(\tau) f_r\left(\frac{L(t)}{L(t_w)}\right). \quad (16)$$

Here $C_{st}(\tau) \simeq L(\tau)^{-2(d-D)}$ and $R_{st}(\tau) \simeq \beta L(\tau)^{-2(d-D)-z_{eq}}$, where $\tau = t - t_w$. The scaling functions f_c and f_r describe the non-equilibrium behavior and take the limiting values $f_c(0) = f_r(0) = 1$ and $f_c(\infty) = f_r(\infty) = 0$. The correlation and response function of the equilibrium state at T_c obey FDT, $R_{st}(\tau) = \beta \dot{C}_{st}(\tau)$. In the scaling forms the equilibrium and non-equilibrium contributions enter in a *multiplicative* structure. Non-equilibrium effects are taken into account by taking ratios between the sizes of the correlated domains at the observation times t_w and t in the scaling functions. Of a certain interest is the limiting fluctuation-dissipation ratio $T/T_{eff} = X_\infty = \lim_{t \rightarrow \infty} \lim_{t_w \rightarrow \infty} = TR(t, t_w)/[\partial C(t, t_w)/\partial t_w]$, due to its universal character (39).

Experiments on the non-equilibrium kinetics near a critical point are reported in (42), where the orientation fluctuations of the director of a liquid crystal are measured after a sudden change of the control parameter (in this case an AC voltage) from a value in the ordered phase to one near the critical point where the Fréedericksz second order transition occurs. In this *quenching* procedure the initial state is ordered. Experimental data show a behavior of two-time quantities in substantial agreement with the scaling pattern described in Eqs. (16), as expected since the system can be described in terms of a time-dependent Ginzburg-Landau equation, similarly to ordinary magnetic systems. Interestingly enough, even the limiting fluctuation-dissipation ratio X_∞ turns out to be in good agreement with the value found in the two-dimensional Ising model.

3.3 Aging in the low-temperature phase

The late stage of phase-ordering in binary systems is characterized by a patchwork of large domains the interior of which is basically thermalized in one of the two equilibrium phases while their boundaries are slowly moving producing the power-law $L(t) \sim t^{1/z}$. This picture suggests the splitting of the degrees of freedom (spins) into two categories, providing statistically independent contributions to observables such as correlation or response functions. More precisely, a quasi-equilibrium stationary contribution arises as due to bulk spins, while boundaries account for the non-equilibrium part. Then (43), asymptotically one has

$$C(r, t) \simeq C_{st}(r) + C_{ag}(r, t) \quad (17)$$

The first term describes the equilibrium fluctuations in the low temperature broken symmetry pure states

$$C_{st}(r) = (1 - \langle s_i \rangle_{eq}^2) g\left(\frac{r}{\xi_{eq}}\right), \quad (18)$$

where $\langle s_i \rangle_{eq}$ is the equilibrium expectation value of the local spin, and $g(x)$ is a function with the limiting values $g(0) = 1$, $\lim_{x \rightarrow \infty} g(x) = 0$. The second term takes into account the motion of the domain walls through

$$C_{ag}(r, t) = \langle s_i \rangle_{eq}^2 f\left(\frac{r}{L(t)}\right), \quad (19)$$

with $f(1) = 1$ and $\lim_{x \rightarrow \infty} f(x) = 0$. Both C_{st} and C_{ag} obey (separately) scaling forms with respect to the equilibrium and the non-equilibrium lengths ξ , $L(t)$. In particular,

Eq. (19) expresses the fact that system configurations at different times are statistically similar provided that lengths are measured in units of $L(t)$, namely the very essence of dynamical scaling.

An analogous *additive* separation holds for two time quantities

$$C(t, t_w) \simeq C_{st}(\tau) + C_{ag}(t, t_w), \quad (20)$$

and similarly for the response function. The equilibrium character of the first term implies

$$C_{st}(\tau) = (1 - \langle s_i \rangle_{eq}^2) g_c \left(\frac{L(\tau)}{\xi_{eq}} \right), \quad (21)$$

where $g_c(x)$ is a function with the limiting values $g_c(0) = 1$, $\lim_{x \rightarrow \infty} g_c(x) = 0$. The non-equilibrium term obeys

$$C_{ag}(t, t_w) = \langle s_i \rangle_{eq}^2 f_c \left(\frac{L(t)}{L(t_w)} \right), \quad (22)$$

with $f_c(1) = 1$ and $\lim_{x \rightarrow \infty} f_c(x) = 0$. In the long t_w limit the two terms in Eq. (20) vary in completely different two-time scales. The first one changes when the second one is fixed to $q_{ea} \equiv \langle s_i \rangle_{eq}^2$, see Eq. (6), at times such that $L(t)/L(t_w) \simeq 1$. In this regime C decays to a plateau at $q_{ea} = \langle s_i \rangle^2$, see Fig. 1.1. The second one varies when the first one has already decayed to zero. The mere existence of the second term is the essence of the aging phenomenon below T_c with older systems (longer t_w) having a slower relaxation than younger ones (shorter t_w). Such a sharp separation of timescales is the hallmark of quenches in the ordered phase, at variance with critical quenches where equilibrium and non-equilibrium contributions are entangled in the multiplicative form (16). Although we have used the terminology of binary systems, the scaling structure discussed insofar is believed to hold quite generally (5) (some exceptions will be discussed below), including systems with more than two low temperature equilibrium phases (as described, e.g. by Potts or clock models) or with a continuous symmetry (i.e. vector $O(N)$ models). Contrarily to the case of critical quenches, however, a systematic expansion method in sub-critical quenches is much more difficult (44) and general results comparable to those at T_c are not yet available. The scaling structure discussed above has been proven analytically only in special cases, such as the one dimensional Ising chain with Glauber dynamics (39; 45) or the Langevin dynamics of the d -dimensional $O(N)$ model with non-conserved order parameter in the large N limit (46). It is supported by semi-analytical arguments in two dimensions (47; 48), numerical simulations (50; 51) and approximate theories (53). It has also been confirmed in experiments (54).

The growing length. The growing length depends on a few characteristics of the ordering process – the dimension of the order parameter, whether there are conservation laws, the presence of quenched disorder – and may serve to classify systems in classes akin to universality ones (5). Although the following results are hard to obtain with rigorous arguments, they are by now well established. Basically, one distinguishes two important cases: in clean models $L(t) \simeq t^{1/z}$; in problems with quenched randomness,

where topological defects are pinned, the growing length is expected to slow down from a power law to a logarithmic dependence on time (due to thermal activation above barriers with a power-law distribution) see Sect. 4. The dynamic exponent z depends on the type of microscopic dynamics and dimension of the order parameter. For example, in curvature driven growth with scalar order parameter $z = 1/2$ and in phase separation with scalar order parameter (and no hydrodynamics) $z = 1/3$. A crossover at a static length explains how the activated scaling can be confused with a temperature-dependent power law in dirty cases (55) as explained in Sect. 4.

The scaling functions. The full theoretical description of a coarsening process necessitates the determination of the scaling functions. This is a hard task and there is no powerful and systematic method to attack this problem yet.

Still, Fisher and Huse proposed that the scaling functions in the aging regime, e.g. f_c , should be robust (1). Changes in the model definition that do not modify the nature of the equilibrium initial nor target ordered state – such as weak quenched disorder not leading to frustration – should not alter the scaling functions. This is the so-called *super-universality hypothesis*. In this way the scaling functions in spin models with random ferromagnetic bonds or random fields should be identical to those found in the pure limit. Numerical tests in $d > 1$ systems point in the direction of validating this hypothesis (48; 49; 51) while very recent studies of the scaling properties of the linear response in the $d = 1$ random bond ferromagnet tend to falsify it (52).

The four-point correlation G_4 . The behavior of G_4 , and the way $L(t)$ is encoded in it, can be easily understood in coarsening systems. In Fig. 3.3 a configuration of the system with two interfaces (denoted 1 and 2, continuous lines) at time t_w is sketched. The dashed interface denoted as 3 is the location of interface 2 at the later time t (such that $t - t_w < t_w$). For $t - t_w \ll t_w$ one has $C_i(t, t_w) = 1$ – for concreteness we think in terms of Ising spins – everywhere except in the regions spanned by an interface in the interval (t_w, t) – the region between 2 and 3 in Fig. 3.3 – where $C_i(t, t_w) = -1$. Hence G_4 decays on a volume of order $L^d(t) - L^d(t_w)$ which grows in time, and ξ_4 increases. For longer time differences ($t - t_w \gtrsim t_w$), however, another interface present at t_w (1 in the sketch) may superseed at time t the position of interface 2 at the previous time t_w . From this time on, χ_4 stops growing and saturates to a value of order $L^d(t_w)$, namely the typical volume contained between two interfaces at t_w (i.e. between 1 and 2). The saturation can also be explained by observing that for long time differences, $t - t_w \gg t_w$, χ_4 factorizes as $(1/N) \sum_{i,j} \langle s_i(t) s_j(t) \rangle \langle s_i(t_w) s_j(t_w) \rangle$. Enforcing scaling, $\langle s_i(t) s_j(t) \rangle \simeq f[r/L(t)]$, one recovers $\lim_{t-t_w \rightarrow \infty} \chi_4(t, t_w) \propto L^d(t_w)$. In this way, $L(t_w)$ can be extracted from the long $t - t_w$ behavior of χ_4 but, of course, this is not really necessary in such coarsening problems. Importantly enough, $L(t)$ is a measure of growth of static order in these cases.

Exceptional cases: breakdown of dynamic scaling. There are also a number of coarsening systems in which dynamic scaling breaks down (5). Among these are the XY model [$O(2)$ symmetry] in one (56) and two (57) dimensions, the clock model with $p > 4$ states (58), the one-dimensional Heisenberg model [$O(3)$ symmetry] (59) and the large- N model with conserved dynamics (60). Interestingly, in most cases this is

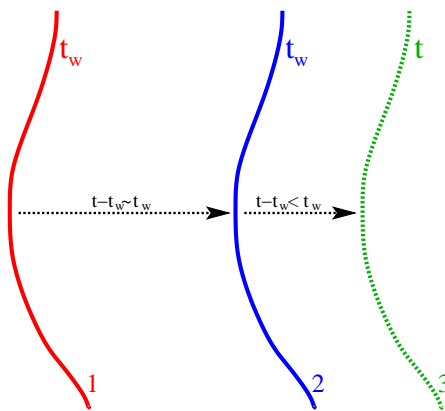


Fig. 3.3 Schematic representation of the mechanism of growth and saturation of $\chi_4(t, t_w)$ in coarsening systems.

due to the presence of more than one length growing macroscopically during phase ordering. Let us consider the XY model in $d = 1$ as a simple paradigm. The order parameter in this case is a planar vector. For long times after a quench from a high to zero temperature, when the excess energy is greatly reduced, the continuous nature of the order parameter allows only soft (Goldstone) modes, namely smooth rotations of the order parameter, called textures. A winding length L_w can be defined as the typical distance over which a 2π rotation of the spin is detected. In addition, due to the symmetry of the disordered initial state and of the Hamiltonian between clockwise (textures) and counterclockwise (anti-textures) rotations, both topological defects are formed in the evolution, separated by winding inversions. Denoting with L the typical distance between winding inversions, it is clear that the reduction of energy implies the growth of both L_w and L as time elapses. It was shown (56) that these lengths grow with different exponents and this phenomenon prevents dynamic scaling to set in.

3.4 Elastic manifolds

The dynamics of a directed d -dimensional elastic manifold embedded in an N dimensional transverse space is simply modeled by a Gaussian scalar field theory that goes under the name of Edwards-Wilkinson (EW) model. Non-linear effects can be accounted for by including a Kardar-Parisi-Zhang (KPZ) term. It has been known for some time that these systems age and that the aging dynamics is governed by a growing correlation length (5; 16; 61; 62).

The aging regime, before saturation at a time-difference that depends on the length of the line, L , is characterized by a multiplicative scaling of two-time quantities. For instance, a two-time generalization of the roughness, $\langle w^2 \rangle(t, t_w) \equiv L^d \int d^d x [\delta h(\vec{x}, t) -$

$\delta h(\vec{x}, t_w)]^2\rangle$, with $\delta h(\vec{x}, t) = h(\vec{x}, t) - \langle h(\vec{x}, t) \rangle$, h the height of the manifold and \vec{x} the position on the d -dimensional substrate, scales as

$$\langle w^2 \rangle(t, t_w) \simeq L^{2\zeta}(t_w) f_{w^2} \left(\frac{L(t)}{L(t_w)} \right). \quad (23)$$

Assuming $\lim_{x \rightarrow \infty} f_{w^2}(x) = x^{2\zeta}$, in the limit $\tau \gg t_w$ this observable reaches a stationary regime in which $\langle w^2 \rangle(t, t_w) \simeq L^{2\zeta}(\tau)$. For even longer time-delays such that $L(t) \rightarrow L$ one finds saturation at $L^{2\zeta}$. The roughness exponent ζ is due to thermal fluctuations and it is simply equal to $(2 - d)/2$ in the EW manifold. The cross-over to saturation is then described by an extension of the Family-Vicsek scaling that takes into account the out of equilibrium relaxation and aging effects. Correlation and response functions are related by a modified fluctuation-dissipation relation after removing the diffusive factor and a well-defined effective temperature (38) exists and depends on the initial (T_0) and final (T) values of the temperature before and after the quench with $T_{eff} > T$ if $T_0 > T$ and $T_{eff} < T$ if $T_0 < T$ (61; 62).

4 Role of activation: the droplet theory

The dynamics of glassy systems at low enough temperatures should be dominated by thermal activation. Although it is very difficult to study activated processes from first principles, several phenomenological proposals for models with quenched disorder exist. In particular, a droplet picture has been put forward for spin-glasses (1; 63; 64) and related systems including elastic manifolds in random media (65) and vortex glasses (66). This model assumes that a static low temperature phase, associated with a zero temperature glassy fixed point in a renormalization group sense, exists in these systems. Droplet-like low-energy excitations of various sizes L on top of the ground state render the dynamics strongly heterogeneous both in space and time. The typical free-energy gap of a droplet with respect to the ground state and the free-energy barrier to nucleate a droplet are assumed to scale as L^θ and L^ψ , respectively, with θ and ψ two non-trivial exponents. Static order is assumed to grow as in standard coarsening systems. Dynamical observables such as the two-time auto-correlation function should then follow universal scaling laws in terms of a growing length $L(t)$ originated in Arrhenius activation over barriers growing as a power of the length

$$t \sim \tau_0 e^{\frac{L^\psi}{T}} \quad \Rightarrow \quad L(t) \simeq [T \ln(t/\tau_0)]^{1/\psi}. \quad (24)$$

The strong-disorder renormalization approach in configuration space (67) yields an explicit construction in favor of the droplet logarithmic scaling.

In the case of spin-glasses the very existence of static glassy states is accepted but their detailed nature is a much debated issue. Moreover, it is far from obvious whether coarsening of only two competing states occurs and whether the growth is determined by thermal activation over such barriers. In the present section we discuss a recipe to examine the droplet picture quantitatively.

4.1 Efficient strategy for data analysis

In practice, the asymptotic dynamic scaling features associated with the putative zero temperature glassy fixed point are difficult to access in numerical simulations

and experiments. The following strategy helps avoiding the control of pre-asymptotic effects that last for very long (68):

- I) Measure the dynamical length $L(t)$ and analyze it over the full time duration by taking care of the crossover from the initial non-activated dynamics, that could be diffusive, critical or else, to the asymptotic activated regime.
- II) Reparametrize the time-dependent quantity of interest, say $A(t)$, using $L(t)$ obtained in I) as a time-length dictionary.

In this way pre-asymptotic corrections are dealt with separately: those due to L and those due to the scaling functions. Once the ‘dictionary’ $L(t)$ is determined, step-II) is very much straightforward: no uncontrolled fits are needed since the essential exponents (such as the energy exponent θ) are provided by independent studies of static properties. We prove the efficiency of this strategy by analysing numerical results for Sinai diffusion (70) and we recall the study of the random manifold and Edwards-Anderson spin-glass along these lines.

Sinai model: a test case. The Sinai model is a random walker hopping on a one-dimensional lattice $i = 1, 2, \dots, N$ over which a quenched random potential U_i is defined. The statistics of the random potential are such that $[(U_i - U_j)^2] = r_{ij}$ where r_{ij} is the distance between sites i and j and $[\dots]$ stands for the average over different realizations of the random potential. The statistical analysis of disorder yields $\theta = \psi = 1/2$.

The walker starts from a randomly chosen initial point at time $t = 0$. The mean-squared displacement is $B(t, t_w) = [\langle (x(t) - x(t_w))^2 \rangle]$ with $x(t)$ the position at time t and $\langle \dots \rangle$ an average over thermal histories and initial conditions. The rigorous analysis of $\sqrt{B(t, 0)} = L(t)$ gives the diffusion law $L(t) \propto [T \ln(t/\tau_0)]^2$ at temperature T (70). Also of interest is the linear-susceptibility, $\chi(t, t_w)$, of the averaged position with respect to a small bias field acting on the walker after the waiting time t_w . In equilibrium the FDT relates the two quantities as $\chi(t, t_w) = B(t, t_w)/2T$.

The asymptotic scaling properties have been almost fully uncovered by a real-space renormalization group (RSRG) approach (71) which is believed to become exact asymptotically. For illustrative purposes, we reproduce some of these results with droplet scaling arguments.

In the quasi-equilibrium regime $L(\tau = t - t_w) < L(t_w)$ the RSRG predicts $B(\tau + t_w, t_w) = 2T\chi(\tau + t_w, t_w) \sim TL^{3/2}(\tau)g_b(L(\tau)/L(t_w))$ where g_b is a scaling function. The exponent $3/2$ can be explained as follow. In first approximation at time t_w the particle sits in the lowest energy minimum within a length scale $L(t_w)$ around the initial point. Since $L(\tau) \ll L(t_w)$ the particle does not have time to explore regions which are far from this minimum and diffusion typically vanishes in the quasi-equilibrium regime. However, with a small probability $\delta U_H/L^\theta(\tau) \sim T/L^\theta(\tau)$ with $\theta = 1/2$ there is a secondary energy minimum within the length scale $L(\tau)$ with the energy barrier between them being lower than the thermal energy T . In such a rare event the particle can hop to the secondary minimum yielding the disorder-averaged behaviour $B(\tau) \simeq T/L^{1/2}(\tau)L^2(\tau) \simeq TL^{3/2}(\tau)$.

In the aging regime $L(t) > L(t_w)$ the particle diffuses over longer and longer lengths looking for lower and lower energy minima. Within a given time scale t the particle

moves to the right or to the left by an amount $L(t)$. However, the direction of motion is almost deterministically given by the direction with the lowest energy barrier since the difference between energy barriers (not minima) is of order $L^{1/2}(t)$, a diverging quantity in the long times limit. One then has $B(t, t_w) \sim L^2(t) f_b(L(t)/L(t_w))$. This also implies that the linear susceptibility typically vanishes in the aging regime since a change of the potential of order $\delta U_H = hL(t)$ (an analogue of the Zeeman energy in magnets) induced by an *infinitesimal* field h does not affect the difference in energy barriers of order $L^{1/2}(t)$. However, there are rare events such that the energy barriers to the left and right are almost degenerate with only a small difference in height δU_H . The probability to find such degenerate barriers scales as $\delta U_H/L^\psi$ with $\psi = 1/2$. The infinitesimal h then induces a change in the direction of diffusion resulting in a disorder-averaged displacement of order $(\delta U_H/L^\psi)L$ and thus $\chi(t, t_w) \sim L^{3/2}(t) f_\chi(L(t)/L(t_w))$.

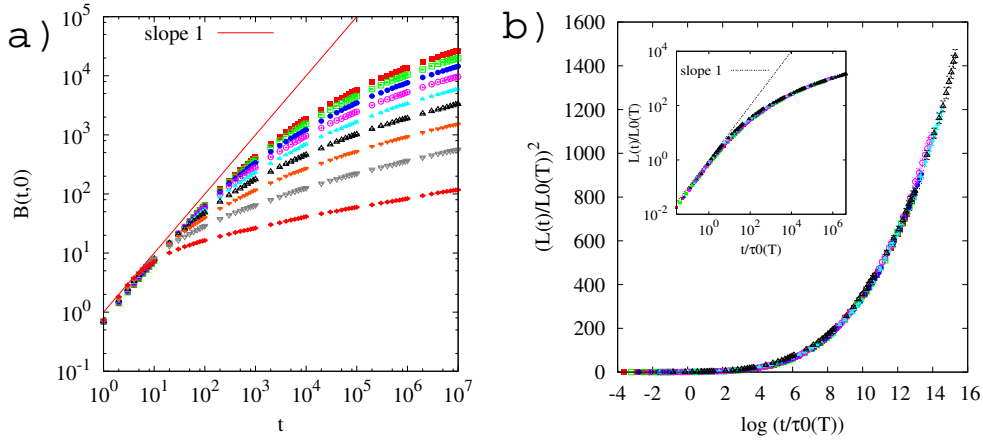


Fig. 4.4 Diffusion in the Sinai model: the mean-squared displacement from MC simulations. a) Raw data at $T = 1.8, 1.6, \dots, 0.4, 0.2$ from top to bottom. The unit of time t is one MCs. The average is taken over 10^5 realizations of the random potential. b) Scaling plot of the dynamic length $L^2(t) = B(t, 0)$ showing the crossover behaviour from normal diffusion at short time t – see the inset – to the expected $L^2 \simeq \ln^4(t/\tau_0)$ asymptotic law.

We performed Monte Carlo (MC) simulations to examine the anticipated asymptotic scaling (68; 69). In Fig. 4.4 a) we show the mean-squared displacement $B(t, 0)$ of the Sinai walker at different temperatures, decreasing from top to bottom. It defines unambiguously a dynamical length $L(t) = \sqrt{B(t, 0)}$ that we shall use below to reparametrize time dependent quantities. The data demonstrate that extremely long times are needed to reach the $L(t) \simeq \ln^2 t/\tau_0$ asymptotic result known to be exact analytically. At finite T the short-time diffusion is normal $B(t, 0) = Dt$ with a diffusion constant D , see the inset in Fig. 4.5. The crossover to the activated regime takes place at a ‘thermal length scale’ $L_0(T)$ such that $\delta U(L_0(T)) = L_0^{1/\theta}(T) \sim T$ and the corresponding time scale $\tau_0(T)$ is fixed using $L_0^2(T) = D\tau_0(T)$. As shown in Fig. 4.4

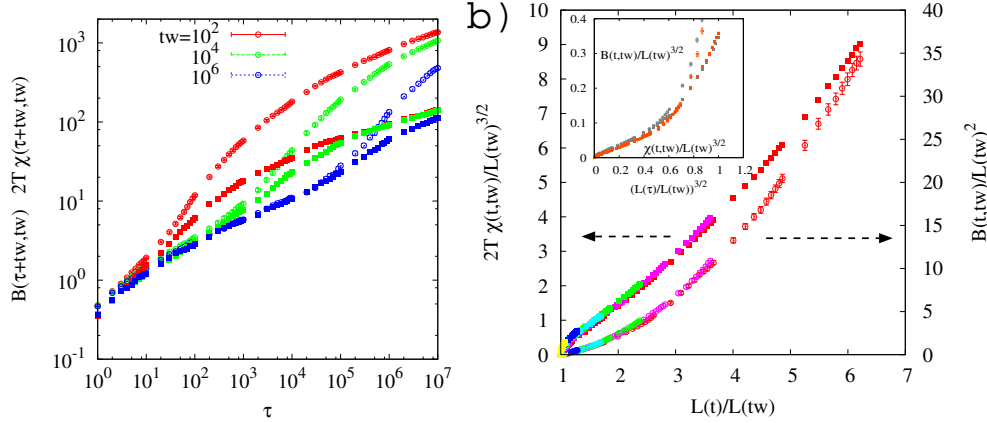


Fig. 4.5 Diffusion in the Sinai model: two-time mean-squared displacement and linear susceptibility from MC simulations at $T = 0.6$. Note the absence of a developing plateau. a) Raw data of the mean-squared displacement $B(t, t_w)$ (open symbols) and the linear-susceptibility $\chi(t, t_w)$ (filled symbols). b) Scaling plots in terms of the dynamic length. Inset: zoom over the quasi-equilibrium regime.

b) the slow crossover is well described by proposing that the scaled length $L(t)/L_0(T)$ is a universal function of the scaled time $t/\tau_0(T)$. The asymptotic Sinai's diffusion law can be parametrized precisely with $L(t) \sim L_0(T)[\ln(t/\tau_0(T))]^2$.

Next we proceed to step II). In Fig. 4.5 a) we show the aging effects observed in the mean-squared displacement and the corresponding linear-susceptibility. In Fig. 4.5 b), the numerical data are reparametrized by the dynamical length scale obtained in the step I) and follow the expected scaling laws. This means that the correction to the asymptotic behaviour is not large in terms of length scales. The absence of a plateau in B and χ in their raw and scaled forms demonstrates the fact that there is no additive separation of time-scales – as in Eq. (20) – in this problem.

Elastic manifolds in random media. The dynamics of a directed d -dimensional elastic manifold embedded in an N dimensional transverse space under the effect of a quenched random potential play an important role in a variety of physical systems ranging from coarsening in dirty systems to fracture. An application is the one in which the directed lines are vortices in super-conductors aligned in the direction of the magnetic field and simultaneously pinned by impurities.

These systems are intimately related to the problem of Sinai's diffusion. The simplest case is a 1+1 dimensional directed polymer in random media (DPRM). Each configuration is described by the transverse displacement $x(z, t)$ at position z along the directed polymer at time t . Two natural quantities used to characterize aging are the mean-squared displacement $B(z, t, t_w) = [\langle (x(z, t) - x(0, t_w))^2 \rangle]$ and the linear susceptibility $\chi(z, t, t_w)$. The FDT $\chi(z, t, t_w) = B(z, t, t_w)/2T$ is satisfied in equilibrium.

Scaling arguments of droplet type naturally apply to the present case (68). To this end one just needs to keep in mind the scaling relation between the longitudinal length

L and transverse length $L_\perp \propto L^\zeta$ with ζ the roughness exponent. Depending on the explored length scale, the latter takes a thermal, $\zeta_T = 1/2$ or a disorder, $\zeta_D = 2/3$, value with the crossover given at a static temperature dependent length $L_0(T)$. The disorder-dominated roughness exponent is related to the energy exponent θ by an exact scaling relation $\theta = 2\zeta_D - 1$ implying $\theta = 1/3$. It is also conjectured that $\psi = \theta$. The time evolution of a local segment $x(z, t)$ may be viewed as diffusion of a particle which feels an effective (renormalized) potential created by the rest of the system, the variation of which scales with the transverse length as $\Delta U \simeq L^\theta \simeq L_\perp^{\theta/\zeta_D} \simeq L_\perp^{2-1/\zeta_D}$ in the disorder dominated regime (72).

Using the analogy with the Sinai model one derives the scaling behaviour of different observables. At a time t after the quench, the system is equilibrated up to longitudinal length $L(t)$ over which the energy is higher than the equilibrium one by an amount of order L^θ . Thus the energy density per unit longitudinal length, $e(t) \equiv U(t)/L$, is expected to decay as $e(t) = e(\infty) + ct/L(t)^{1-\theta}$. In the quasi-equilibrium regime the consideration of the degeneracy of minima suggests $B(z, \tau + t_w, t_w) = 2T\chi(z, \tau + t_w, t_w) = TL(\tau)g_b(z/L(t_w), L(\tau)/L(t_w))$ [the prefactor $TL(\tau)$ is due to $T/L^\theta(\tau)L^{2\zeta}(\tau) = TL(\tau)$ since $\theta = 2\zeta - 1$.] In the aging regime we find $B(z, t, t_w) = L(t)^{2\zeta}f_B(z/L(t_w), L(t)/L(t_w))$ while $\chi(z, t, t_w) = L(t)f_\chi(z/L(t_w), L(t)/L(t_w))$ due to the degeneracy of barriers.

In order to test the above, the simplest protocol is to choose a flat initial condition, *i.e.* $x(z, 0) = 0$ for all z . During isothermal aging the roughness of the system develops progressively from short to long wave lengths. The dynamical length $L(t)$ can be extracted from the growth of the static roughness $B(0, t, t) = [\langle (x(z, t) - x(z, 0))^2 \rangle] = B_{eq}(z = L(t))$. Here $B_{eq}(z) = \lim_{t \rightarrow \infty} B(z, t, t)$ is the equilibrium roughness, which can be computed numerically with a transfer matrix method in the 1+1 case (68). Another way to determine $L(t)$ is given in (55).

By performing Monte Carlo simulations of the 1+1 DPRM the analysis of step I) and II) can be done precisely (68; 55) helped by the knowledge of the exact values of the exponents $\zeta_T = 1/2$, $\zeta_D = 2/3$ and $\theta = 1/3$. Quite interestingly the variation of the energy scales as $\Delta U \simeq L_\perp^{1/2}$ just as in the Sinai model discussed before.

Concomitantly with the change in roughness exponent from thermal to disorder dominated values, $L(t)$ exhibits a gradual crossover from pure diffusion with $L(t) \simeq t^{1/z}$ (and $z = 2$) to an activated regime consistent with an algebraic growth of barriers (65). This is similar to what is found in the Sinai model (see Fig. 4.4) but with $\psi = 1/3$. The crossover occurs at a static temperature-dependent correlation length $L_0(T)$. In the analysis of numerical data the two regimes tend to be confused into a single one with an effective temperature-dependent power-law, $L(t) \sim t^{1/\bar{z}(T)}$ (86), the T -dependence of which is inherited from the one in $L_0(T)$ (55), but this is just an approximation. Further support to the asymptotic logarithmic scaling is given by the renormalization group study in (67).

As regards the scaling properties of the two-time quantities $B(z, t, t_w)$ and $\chi(z, t, t_w)$ in the quasi-equilibrium and aging regimes one also faces the difficulty of going beyond the thermal regime and reaching, for sufficiently long time-scales, the disorder dominated one. In (55) it was shown that in the early effective power-law regime, approximated by $L(t) \simeq t^{1/\bar{z}(T)}$, and using the thermal roughness exponent, two-time

linear response and correlation functions conform to the scalings discussed above and a finite effective temperature exists [basically because $2\zeta_T = 1$ and the diffusive prefactors in B and χ are both equal to $L(t)$]. Simulations entering the trully activated regime suggest that the dynamic scaling above with the disorder roughness exponent ζ_D sets in (and the effective temperature progressively vanishes) (68).

Spin glasses. The isothermal aging of the Edwards-Anderson (EA) model was analyzed along the same steps. The model is supposed to have a finite temperature phase transition and thus an additive separation of time-scales of the form (20) – the precise nature of the aging term depending on a two-state droplet picture (1; 63; 64) or a more complicated dynamics of the Sherrington-Kirkpatrick (SK) type (4).

The growing length is extracted from the real-replica overlap, see eq. (14) (25). It is common to use the fit $\xi_{sg}(t) \sim t^{1/\bar{z}(T)}$ with $\bar{z}(T)$ an effective temperature dependent exponent (24; 25; 33; 34; 35). The best currently available data are from the JANUS collaboration suggesting $\bar{z}(T) \simeq \bar{z}(T_c)T_c/T$ (24). However, $\xi_{sg}(t)$ should exhibit a gradual crossover from critical dynamics at short-times to activated dynamics asymptotically (36; 73). The crossover is expected at $L_0(T) \sim \xi$ and $\tau_0(T) \sim \xi^{z_{eq}}$ with the equilibrium correlation length $\xi = |T - T_c|^{-\nu}$ and z_{eq} and ν the usual critical exponents at the critical temperature T_c . The values of T_c , ν , z_{eq} and θ are fixed with equilibrium studies. In the rest of the discussion we call $L(t)$ the growing length [$\xi_{sg}(t) \rightarrow L(t)$].

Similar arguments to the ones exposed for Sinai diffusion and the directed manifold imply that the energy density per spin should decay as $e(t) = e(\infty) + ct/L(t)^{d-\theta}$ and provide scaling forms for the self-correlation and linear susceptibility of very similar type to the ones in previous subsections (but with different values of the exponents).

Numerical tests of the droplet picture predictions were done by a number of groups. The energy density decay in the $d = 3$ and $d = 4$ EA models were checked in (35) and (36), respectively. The numerical spin auto-correlation function $C(t, t_w)$ and the linear susceptibility $\chi(t, t_w)$ were analyzed along the proposed scaling forms. In the quasi-equilibrium regime where the FDT $C(\tau + t_w, t_w) = T\chi(\tau + t_w, t_w)$ holds, the expected scaling $C(\tau + t_w, t_w) = q_{ea} + ct \ T/L(\tau)^\theta g_c(L(\tau)/L(t_w))$ with $g_c(\lambda) \propto 1 - \text{const } \lambda^{d-\theta} + \dots$ was verified in $d = 3$ (35) and $d = 4$ (36) (the fact that $L(t)$ is far from a logarithm was attributed to pre-asymptotics and the analysis was performed using the method sketched above.). Evidence for the validity of droplet aging scaling for the correlation function $C_{ag}(t, t_w) = f_c(L(t)/L(t_w))$ and the field cooled susceptibility in which the sample is cooled in a field that it switched off at t_w , $\chi_{fc}(t, t_w) = \chi(t, 0) - \chi(t, t_w) = L(t)^{-\theta} f_\chi(L(t)/L(t_w))$ with $\chi(t, 0) = \chi_D - \text{const } T/L(t)^\theta$ (1) in $d = 4$ was given in (36) (note that $\psi \simeq \theta$ is assumed here). These results were used as support to the standard droplet theory. However, the asymptotic value of the dynamical susceptibility χ_D is significantly higher than $\chi_{ea} = \beta(1 - q_{ea})$ (36; 34). This is clearly at odds with the standard droplet theory (1) and suggests the existence of excessive contributions from some unknown soft-modes other than the droplets in equilibrium. Moreover, it was found that the FDT holds up to significantly longer time-differences than time-translational invariance (36). These observations suggest that, even within a droplet perspective, modifications of the conventional approach are needed.

A different school of thought (34; 24) pushes for a picture *à la* mean-field (namely, the dynamics of the SK model (4)) that should be accompanied by a complex relaxation of correlations and susceptibilities in multiple time-scales, presumably linked to multiple length-scales. So far, this *ultrametric* organization of time-scales has not been found numerically (21; 24; 87).

4.2 Other random systems

Let us finalize this Section by briefly recalling studies of growing lengths in two other systems with quenched randomness: the random ferromagnet and the sine-Gordon model with random phases.

On the basis of a droplet theory with barriers increasing as a power-law of distance, the random ferromagnet should coarsen with a logarithmically increasing typical length (88). Early Monte Carlo simulations (89) showed agreement with this prediction but more recent numerical results from Rieger’s group were interpreted, instead, as evidence for a power-law with variable exponent (90). This result would imply a logarithmic dependence of barriers on the domain size. It was argued in (55) that the effective power law maybe the effect of a very long crossover from curvature driven to activation with conventional power-law growth of barriers with size. Recent simulations support this claim (91) – although they were performed in a dilute ferromagnet.

The Cardy-Ostlund or random sine-Gordon model describes the relaxation dynamics of $2d$ periodic elastic manifolds under the effect of a quenched random potential. The peculiarity of the model is that disorder induced barriers grow only logarithmically with size, $\simeq \ln L$. A ‘super-rough’ or ‘marginal’ glassy phase exists below a critical temperature T_g . The aging dynamics were studied with Coulomb gas and renormalization methods close to T_g , and with the functional renormalization group (FRG) (92) and numerical simulations in the full low- T phase (93). A dynamic length $L(t) \sim t^{1/z(T)}$ with $z(T) \simeq 2 + c/T$ develops in time, consistently with an Arrhenius argument of the kind described in Sect. 4. Intriguingly, $X_\infty = z$ was also found analytically and numerically.

5 Growing length-scales in aging glasses

In this Section we summarize predictions from mean-field theory as well as the outcome of measurements of two-time lengths in several glassy systems.

5.1 Mean-field models

It has been argued that the Langevin dynamics of mean-field disordered models are equivalent to mode-coupling theories of glasses. More precisely, the Sherrington-Kirkpatrick (SK) spin-glass has a dynamic transition similar to the one found in so-called type A mode-coupling while p -spin models with $p > 3$ have a random-first-order transition (RFOT) similar to the one found in type B mode-coupling theories (82). The asymptotic out of equilibrium relaxation of these models, when the thermodynamic limit has been taken at the outset, approaches a region of phase space that is not the one where equilibrium configurations lie. In models of the RFOT class this region was named the *threshold* since its energy density is at $O(1)$ distance from the equilibrium

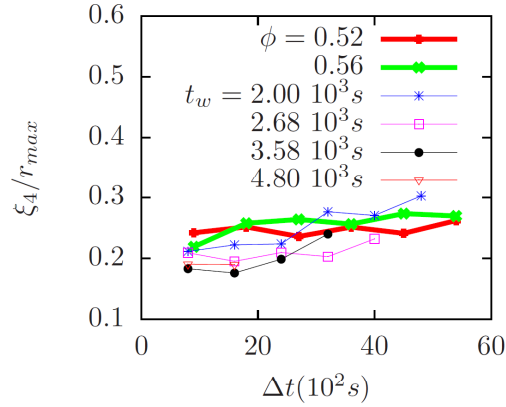


Fig. 5.6 The two-time dependent growing length in a colloidal suspension. The data is taken from (8). ϕ is the packing fraction and r_{max} is a cut-off used to compute the integrals (see (8) for more details).

one (3). In models of the SK or type A class, although the configurations visited dynamically are not the ones of equilibrium their energy density is the same (4). In both cases the region reached dynamically is *flat*, in the sense that a dynamic free-energy landscape can be defined and its geometric properties studied, and one finds that the eigenvalues of its Hessian mostly vanish (3). The flat directions provide, on the one hand, channels of aging relaxation and, on the other, their associated zero-modes give rise to diverging susceptibilities. In the case of mean-field models the latter cannot be directly associated to diverging length-scales since these models do not contain any notion of distance. Having said this, if one proposes that the same mechanism, namely the relaxation to a flat region of phase space, is at the root of aging phenomena in finite dimensional glassy systems, the diverging susceptibility should be linked to a diverging length scale. In the super-cooled liquid regime this argument was used by Franz and Parisi to argue for the existence of a diverging length scale within the RFOT scenario from the analysis of the p -spin model (94), see the chapter by Franz and Semerjian. These ideas were extended to the actual MCT in (95). In the trully glassy phase a very similar mechanism is at work and gives support to the symmetry argument (9) that we discuss in Sect. 6 and provides a scenario for dynamic fluctuations in aging glassy systems.

5.2 Measurements

In Sect. 2.1 we already mentioned simulations (13) and experiments (14) in which the tagged motion of particles was followed with the intention of characterizing clusters of more or less mobile ones in aging glasses.

A two-time dependent dynamic growing length, as defined in Eq. (10), was measured with numerical simulations of aging soft spheres and Lennard-Jones mixtures (20; 83), spin-glasses (15; 21; 24) and with confocal microscopy data of colloidal suspensions (8; 96). An example is shown in Fig. 5.6 where we display the outcome of the data analysis performed in (8).

In all cases ξ_4 is described by

$$\xi_4(t, t_w) \simeq \begin{cases} \xi_{st}(t - t_w) & C > q_{ea} \\ t_w^a \kappa(C) & C < q_{ea} \end{cases}$$

with $\kappa(C)$ a monotonically decreasing function of C and the exponent a taking a very small value. It is important to stress that a clear identification of a finite Edwards-Anderson parameter in some of these systems is hard and the separation of time scales might not be as clear-cut as expressed in the formula above.

5.3 Growth processes in kinetically constrained models

Kinetically constrained models were originally introduced in the 80s by Fredrickson and Andersen (97) as toy models for understanding glassy dynamics. Generally these are stochastic models with Markovian dynamics obeying detailed balance with respect to a (usually) trivial energy function. Some constraints prevent particular local transitions between configurations (98). Despite their trivial equilibrium measure, they capture many features of real glass-forming systems summarized in the chapter by Garrahan, Sollich and Toninelli.

The so-called spin-facilitated Ising models, are described by the Hamiltonian $H = -\sum_i n_i$, where $n_i = 0, 1$ are spin variables on a d -dimensional lattice which can be regarded as a coarse grained density of moving particles. The basic idea is that the rearrangement in a certain region around i will be facilitated if it is surrounded by a relatively low-density neighbourhood. In some of these systems, the existence of a growing length in the non-equilibrium evolution after a quench can be easily recognized. Some time after a sudden change in temperature towards $T \simeq 0$ all sites are in a dense state with $n_i = 1$ and large frozen regions, the size of which increases as the number of sites with $n_i = 0$ decreases, are present (99).

A particularly interesting kinetically constrained system is the $2d$ spiral model. It has the peculiar feature of having a glass-jamming transition at the critical density $\langle n_i \rangle = n_c$ of directed percolation (100). In equilibrium above n_c a finite fraction of sites are frozen by the kinetic constraint. This means that the configuration space is partitioned into mutually inaccessible regions; namely, the dynamics is reducible. Then all configurations without blocked regions are dynamically connected to the empty state with $n_i = 0 \forall i$, usually denoted as the high-temperature partition, and they are disconnected from any partition containing frozen regions. Therefore, quenching the system from (say) the empty state to the jammed phase, the dynamics do not freeze and remain confined in the high temperature partition by means of a coarsening process with a growing correlation length which resembles in some sense the one observed in binary systems without kinetic constraints (101).

5.4 Interplay between aging and drive

The classical and quantum dynamics of large systems under an external, non-conservative, drive is a subject of active research. An example in the first family is the analysis of the rheological properties of soft glassy materials, that are a result of a competition between the response to the shearing forces and their intrinsic slow dynamics. An example in the second class is the study of quantum magnets under a current generated

to the coupling to leads at different chemical potential. We shall recap here and in Sect. 5.6 a few issues in this field that are related to the growth of a length and how this is affected by the drive.

Flow in coarsening systems. The effect of an external drive on coarsening systems is not completely understood and in many cases a general consensus is lacking. This is at odds with the wide technological interest of these and similar systems in various application areas (102). In particular, the case of binary systems in a plane shear flow (Couette flow) has been thoroughly studied recently. In this case domains grow elongated and stretched along the flow direction. This causes ruptures of the network (103) that may render the segregation incomplete. The characteristic lengths in the parallel or perpendicular directions to the flow could keep on growing indefinitely as without shear or, due to domain break-up, the system may eventually enter a stationary state (similarly to what happens in the mean field models discussed above) characterized by domains with a finite thickness. In general, there is no agreement on this point neither from experimental (104) nor theoretical points of view. On the theoretical side, large- N calculations (105) show the existence of an asymptotic regime with ever growing lengths in all directions. Stabilization of the domain size by rupture is excluded also by different approaches based on approximate theories for scalar systems complemented with RG analysis (106), although with the unexpected feature of domains growing in the flow direction while shrinking in the perpendicular one in $d = 2$. Numerical simulations (107) cannot still establish a clear-cut evidence due to finite size and discretization effects. It was also argued (108) that hydrodynamic effects are crucial in stabilizing a stationary state, while in the diffusive regime domains might keep on growing.

Another difference with driven mean-field models is provided by the fluctuation-dissipation relation $\chi(C)$, the exact computation of which in the large- N model (109) excludes a simple scenario with a single effective temperature. Much more details are given in the contribution by Barrat and Lemaître.

Flow in glassy systems. The Langevin dynamics of mean-field disordered models under non-potential forces has been studied in a series of papers (110; 53). In all cases (apart from the spherical model with two-body interactions at zero temperature) aging is suppressed and a stationary state is reached. Two-time observables decay in two steps and the relaxation time decreases with the strength of the drive as in shear thinning systems. In the limit of weak drive the effective temperature takes two values, the one of the bath in the first relaxation step and a higher value in the second slower stage. These results have been verified in molecular dynamic simulations of Lennard-Jones mixtures (111).

The fact that a weak non-potential perturbation can change the relaxation of a classical system so dramatically, by rendering the dynamics stationary, can be understood in different ways. First, the type of non-potential force used in (110) can be loosely associated to an infinite temperature noise. Second, and more importantly, the mechanism for fluctuations based on time-reparametrization invariance gives a reason for this fact, as discussed in Sect. 6.

Experimentally, the interplay between aging and flow in an aqueous suspension of

Laponite has been studied by diffusive wave spectroscopy (112) and light scattering echo experiments (113) (multiple scattering) and dynamic light scattering in the single-scattering regime (114). Using the latter technique Di Leonardo *et al* measured the density auto-correlation function and found that as long as the characteristic relaxation time is smaller than the inverse shear rate aging is unaffected by the perturbation but, when the relaxation time reaches the inverse shear rate, aging is strongly reduced.

A recent study of microscopic structural relaxation of colloidal suspensions under shear together with relevant references appeared in (115). Numerical studies of aging and plastic deformations have been performed by several groups, see the reviews in (116; 117). Nevertheless, as far as we know, an analysis of growing dynamic lengths, as defined from G_4 or χ_4 has not been performed in driven systems yet.

Aging at the depinning transition of elastic manifolds. A series of analytic and numerical papers have recently showed that a non-steady critical regime, limited only by the steady correlation length or the system size, exists at the zero-temperature depinning transition of an elastic manifold in a disordered medium (118). The FRG analysis (92) as well as molecular dynamics studies prove that there is a driven transient aging regime that displays universal features in which a growing length $L(t) \sim t^{1/z}$ participates in the critical dynamic scaling description of the dynamics. At the depinning transition the effective height of the barriers vanishes justifying the power-law scaling the effect of disorder being a reduction of z to a value smaller than 2 (at the existent one-loop FRG calculation).

5.5 Granular matter

The gently driven dynamics of dense granular matter – athermal systems – shows many points in common with the ones of glass forming liquids (119). Aging in a water-saturated granular pile submitted to discrete taps has been reported in (120). The data were obtained using multispeckle diffusive wave spectroscopy to measure particle displacements. Evidence for dynamic heterogeneities and a growing correlation length in a horizontally vibrated amorphous assembly of hard disks close to the jamming transition was given in (121). Presumably, a two-time growing length would also exist in such athermal systems if studied in the aging regime. On the theoretical side, the aging properties of a periodically perturbed mean-field model of the RFOT type and, more precisely, how these depend on the amplitude and frequency of the drive were studied in (122).

5.6 Quantum fluctuations

The study of the dynamics of quantum systems has been recently boosted by the development of cold atom experiments and advanced measurement techniques. Quantum magnets are expected to undergo coarsening dynamics in the ferromagnetic phase. The study of a mean-field model (freely relaxing and driven by an external current) has revealed an extension of the super-universality hypothesis to the quantum realm once small scales are well separated from large ones, the former feeling the quantum fluctuations and the latter describing the motion of large objects – the walls – being basically identical to the classical ones. More precisely, in $O(N)$ field theory in the

large N limit or models of rotors in interaction the length over which static order is established grows as $L(t) \sim t^{1/z}$ with $z = 2$ as in the classical limit. This type of coarsening survives the application of a voltage difference by two leads at different chemical potential (123). This prediction is open to experimental tests.

6 A mechanism for dynamic fluctuations

In a series of papers Chamon *et al* proposed that the symmetry that captures the universal aging dynamics of glassy systems is the invariance of an effective dynamical action under *uniform reparametrizations of the time scales* (15; 21; 30; 31; 32), see also (124). This approach is reviewed in (9). Such type of invariance was first encountered in the *mean-field equilibrium dynamics* of spin-glasses (125; 126) and it was later found in the better formulated *out of equilibrium* dynamic of the same models (3; 4). The invariance means that in the asymptotic regime of very long times the solution can be found up to a time-reparametrization transformation. Within such a scenario, extended to systems in finite dimensions, the remaining symmetry is responsible of the dynamic fluctuations. Support to this claim was given by the proof of global time reparametrization invariance in the long times *action* of *short-range spin-glasses* (30; 15). In the proof one assumes that the dynamics is causal and that there is an additive separation between a time regime with a fast relaxation and another in which it is slow [just as in Fig. 1.1 and in Eq. (20)]. The invariance can then be used to describe dynamic fluctuations in spin-glasses and, as conjectured, in other glassy systems as well. The fact that the dynamic action be symmetric under uniform, *i.e.* spatially independent, reparametrizations of time variables $[t \rightarrow h(t)]$ suggests that the dynamic fluctuations that cost little action are those associated to space dependent, long wavelength, reparametrizations of the form $t \rightarrow h(\vec{r}, t)$. These should be the Goldstone modes associated with breaking time-reparametrization invariance symmetry.

In the slow and aging regime the two-time correlation and linear response depend on both times and time-translation invariance is lost. As we argued in Sect. 1 the two-time dependent correlation acts as an order parameter. Dynamic fluctuations are such that *ages* can fluctuate from point to point in the sample with younger and older pieces (lower and higher values of the correlation) coexisting at the same values of the two laboratory times: this has been named *heterogeneous aging*. By looking now at spatially heterogeneous reparametrizations, we can predict the behavior of local correlations and linear susceptibilities and the relations between them. Different sites can be retarded or advanced with respect to the global behaviour but they should all have the same overall type of decay. Similarly, the relation between local susceptibilities and their associated correlations should be identical all over the sample (15) leading to a uniform effective temperature (38). The reason why the scaling functions should not fluctuate much is that these are massive modes. Within the time-reparametrization invariance scenario the growing correlation length is due to the approach to the long-time regime in which the symmetry is fully developed, and the long wavelength modes eventually become massless.

This hypothesis was put to the test in glassy systems with Monte Carlo simulations of the Edwards-Anderson model (15; 21), molecular dynamics of Lennard-Jones mixtures (83), numerical studies of kinetically constrained models (31), and in the study

of solvable ferromagnetic models with the analysis of the $O(N)$ model in the large N limit (32) and the spherical ferromagnet (84). A series of stringent tests some of them performed in these papers were summarized in (9). The outcome of these studies is that while truly glassy systems conform to the consequences of the hypothesis, simple coarsening as developed in the $O(N)$ and spherical ferromagnet does not with time-reparametrization invariance being reduced to time rescaling at the heart of the difference. This result is very suggestive since it implies that the invariance properties and the fluctuations associated to them are intimately related to the behavior of the global effective temperature (finite against infinite) in the aging regime.

In short, this idea proposes a *reason* for the development of large dynamic fluctuations in glassy dynamics.

7 Closing remarks

In aging systems, the relaxation of typical features in a sample of a certain age t_w takes a time that increases with t_w . Although the reason for this fact is not necessarily the growth of those features, the widespread observation of growing lengths in physical systems, as reviewed in this chapter, promotes this one as the basic mechanism at the heart of most aging phenomena. (See (127) and the chapter by Franz and Semerjian for rigorous relations between growing lengths and growing times.) Related to this fact, the occurrence of dynamic scaling provides a parametrization of the kinetics in terms of typical lengths, giving access to universal properties.

Besides these unifying concepts, the very nature of the growing length, the growth mechanisms, the relation with equilibrium properties *etc.* are issues which, in most cases, deserve clarification. In particular, the interplay between the growth of static order – as, in coarsening systems – and purely dynamical correlations – as in most kinetically constrained models – could help in understanding the behavior of glasses. In the case of spin glasses, moreover, the comprehension of the kind of order established within the correlated volume is fundamental to distinguish between competing scenarios, namely droplet-like and *à la* mean field pictures.

References

- (1) D. S. Fisher and D. A. Huse, Phys. Rev. B **38**, 373 (1988).
- (2) J.-P. Bouchaud, J. Phys. I **2**, 1705 (1992). J.-P. Bouchaud and D. S. Dean, J. Phys. (France) I **5**, 265-286 (1995).
- (3) L. F. Cugliandolo and J. Kurchan, Phys. Rev. Lett. **71**, 173 (1993).
- (4) L. F. Cugliandolo and J. Kurchan, J. Phys. A **27**, 5749 (1994).
- (5) A. J. Bray, Adv. Phys. **43**, 357 (1994).
- (6) Two reviews on different properties of elastic manifolds that do not, however, deal with their aging properties are: A.-L. Barabási and H. E. Stanley, *Fractal Concepts in Surface Growth* (Cambridge University Press, Cambridge, 1995). T. Halpin-Healey and Y.-C. Zhang, Phys. Rep. **254**, 215 (1995).
- (7) E. Donth, *The glass transition: relaxation dynamics in liquids and disordered materials* (Springer, 2001). K. Binder and W. Kob, *Glassy materials and disordered solids: An introduction to their statistical mechanics*, (World Scientific, Singapore, 2005).
- (8) C. Chamon, L. F. Cugliandolo, G. Fabricius, J. L. Iguain, and E. R. Weeks, PNAS **105**, 15263 (2008).
- (9) C. Chamon and L. F. Cugliandolo, J. Stat. Mech. (2007) P07022.
- (10) C. Bennemann, C. Donati, J. Baschnagel, and S.C. Glotzer, Nature (London) **399**, 246 (1999). W. Kob, C. Donati, S. J. Plimpton, P. H. Poole, and S. C. Glotzer, Phys. Rev. Lett. **79**, 2827 (1997). D. Perera and P. Harrowell, Phys. Rev. E **54**, 1652 (1996). C. Donati et al., Phys. Rev. E **60**, 3107 (1999). A. Onuki and Y. Yamamoto, J. Non-Cryst. Solids **235-237**, 19 (1998). B. Doliwa and A. Heuer, J. Non-Cryst. Solids **307**, 32 (2002). A. Heuer, M. Kunow, M. Vogel, and R.D. Banhatti, Phys. Rev. B **66**, 224201 (2002).
- (11) A. van Blaaderen and P. Wiltzius, Science **270**, 1177 (1995). W. K. Kegel and A. van Blaaderen, Science **287**, 290 (2000). E. R. Weeks and D.A. Weitz, Phys. Rev. Lett. **89**, 095704 (2000). E. R. Weeks, J. C. Crocker, A. C. Levitt, A. Schofield, and D. A. Weitz, Science **287**, 627 (2000).
- (12) H. Miyagawa, Y. Hiwatari, B. Bernu, and J-P Hansen, J. Chem. Phys. **88**, 3879 (1988).
- (13) K. Vollmayr-Lee, J. Chem. Phys. **121**, 4781 (2004). K. Vollmayr-Lee and A. Zippelius, Phys. Rev. E **72**, 041507 (2005). K. Vollmayr-Lee and E. A. Baker, Europhys. Lett. **76**, 1130 (2006).
- (14) R. Courtland and E. R. Weeks, J. Phys.: Cond. Matt. **15**, S359 (2003). E. R. Weeks, J. C. Crocker, and D. A. Weitz, J. Phys.: Cond. Matt. **19**, 205131 (2007).
- (15) H. E. Castillo, C. Chamon, L. F. Cugliandolo, and M. P. Kennett, Phys. Rev. Lett. **88**, 237201 (2002), H. E. Castillo, C. Chamon, L. F. Cugliandolo, J. L. Iguain, and M. P. Kennett, Phys. Rev. B **68**, 134442 (2003).

- (16) L. F. Cugliandolo, J. Kurchan, and G. Parisi, J. Phys. I (France) **4**, 1641 (1994).
- (17) E. Lippiello, F. Corberi, and M. Zannetti, Phys. Rev. E **71**, 036104 (2005).
- (18) See, however, the recent proposal in J. Kurchan and D. Levine, *Correlation length for amorphous systems*, arXiv:0904.4850.
- (19) M. Mézard, G. Parisi, and M. A. Virasoro, *Spin glasses and beyond* (World Scientific, 1987).
- (20) G. Parisi, J. Chem. Phys. B **103**, 4128 (1999).
- (21) L. D. C. Jaubert, C. Chamon, L. F. Cugliandolo, and M. Picco, J. Stat. Mech. (2007) P05001.
- (22) G. Semerjian, L. F. Cugliandolo, and A. Montanari, J. Stat. Phys. **115**, 493 (2004).
- (23) E. Lippiello, F. Corberi, A. Sarracino, and M. Zannetti, Phys. Rev. B **77**, 212201 (2008); Phys. Rev. E **78**, 041120 (2008).
- (24) F. Belletti *et al*, Phys. Rev. Lett. **101**, 157201 (2008); J. Stat. Phys. **135**, 1121 (2009).
- (25) D. A. Huse, J. Appl. Phys. **64**, 5776 (1988); Phys. Rev. B **43**, 8673 (1991).
- (26) J.-P. Bouchaud and G. Biroli, Phys. Rev. B **72**, 064204 (2005).
- (27) L. Berthier, G. Biroli, J.-P. Bouchaud, L. Cipelletti, D. El Masri, D. L'Hôte, F. Ladieu, and M. Pierno, Science **310**, 1797 (2005).
- (28) see, e.g. F. Ladieu, C. Thibierge, and D. L'Hôte, J. Phys.: Condensed Matter **19**, 205138 (2007). C. Thibierge, D. L'Hôte, F. Ladieu, and R. Tourbot, Rev. of Scientific Inst. **79**, 103905 (2008).
- (29) F. Corberi, E. Lippiello, A. Sarracino, and M. Zannetti, J. Stat. Mech. P04003 (2010).
- (30) C. Chamon, M. P. Kennett, H. E. Castillo, and L. F. Cugliandolo Phys. Rev. Lett. **89**, 217201 (2002). H. E. Castillo, Phys. Rev. B **78**, 214430 (2008).
- (31) C. Chamon, P. Charbonneau, L. F. Cugliandolo, D. R. Reichman, and M. Sellitto, J. Chem. Phys. **121**, 10120 (2004).
- (32) C. Chamon, L. F. Cugliandolo, and H. Yoshino, J. Stat. Mech (2006) P01006.
- (33) H. Rieger, J. Phys. A **26**, L615 (1993). H. Rieger, B. Steckemetz, and M. Schreckenberg, Europhys. Lett. **27**, 485 (1994). J. Kisker, L. Santen, M. Schreckenberg, and H. Rieger, Phys. Rev. B **53** 6418 (1996).
- (34) E. Marinari, G. Parisi, F. Ricci-Tersenghi, and J. J. Ruiz-Lorenzo, J. Phys. A **33**, 2373 (2000).
- (35) T. Komori, H. Takayama, and H. Yoshino J. Phys. Soc. Japan **68** 3387 (1999); *ibid* **69**, 1192 (1999); *ibid* **69** (Suppl. A) 228 (2000).
- (36) H. Yoshino, K. Hukushima, and H. Takayama, Phys. Rev. B **66**, 064431 (2002).
- (37) A. Crisanti and F. Ritort, J. Phys. A **36**, R181 (2003).
- (38) L. F. Cugliandolo, J. Kurchan, and L. Peliti, Phys. Rev. E **55**, 3898 (1997).
- (39) C. Godrèche and J. M. Luck, J. Phys. A **33**, 9141 (2000); J. Phys.: Condens. Matter **14**, 1589 (2002).
- (40) H. K. Janssen, B. Schaub, and B. Schmittman, Z. Phys. B Cond.Mat. **73**, 539 (1989). P. Calabrese and A. Gambassi, Phys. Rev. E **65**, 066120 (2002); Phys. Rev. E **67**, 36111 (2002); J. Phys. A: Math. Gen. **38**, R133 (2005).
- (41) C. Chatelain, J. Stat. Mech. (2004) P06006. M. Pleimling and A. Gambassi,

- Phys. Rev. B **71**, 180401 (2005). P. Mayer, L. Berthier, J. P. Garrahan, and P. Sollich, Phys. Rev. E **68**, 016116 (2005). E. Lippiello, F. Corberi, and M. Zannetti, Phys. Rev. E **74**, 041113 (2006). M. Henkel, T. Enss, and M. Pleimling, J. Phys. A **39**, L589 (2006). F. Corberi, A. Gambassi, E. Lippiello, and M. Zannetti, J. Stat. Mech. (2008) P02013.
- (42) S. Joubaud, B. Percier, A. Petrosyan, and S. Ciliberto, Phys. Rev. Lett. **102**, 130601 (2009).
- (43) J.-P. Bouchaud, L. F. Cugliandolo, J. Kurchan, and M. Mézard, in *Spin Glasses and Random Fields*, edited by A. P. Young (World Scientific, Singapore, 1997). S. Franz and M. A. Virasoro, J. Phys. A: Math. Gen. **33**, 891 (2000).
- (44) G. Mazenko, Phys. Rev. E **69**, 0116114 (2004).
- (45) E. Lippiello and M. Zannetti, Phys. Rev. E **61**, 3369 (2000).
- (46) F. Corberi, E. Lippiello, and M. Zannetti, Phys. Rev. E **65**, 046136 (2002).
- (47) J. J. Arenzon, A. J. Bray, L. F. Cugliandolo, and A. Sicilia, Phys. Rev. Lett. **98**, 145701 (2007). A. Sicilia, J. J. Arenzon, A. J. Bray, and L. F. Cugliandolo, Phys. Rev. E **76**, 061116 (2007).
- (48) A. Sicilia, J. J. Arenzon, A. J. Bray, and L. F. Cugliandolo, EPL **82**, 10001 (2008).
- (49) M. Henkel and M. Pleimling Phys. Rev. B **78**, 224419 (2008).
- (50) F. Corberi, E. Lippiello and M. Zannetti, Phys. Rev. E **68**, 046131 (2003); Phys. Rev. E **74**, 041106 (2006).
- (51) C. Aron, C. Chamon, L. F. Cugliandolo, and M. Picco, J. Stat. Mech. (2008) P05016.
- (52) E. Lippiello, A. Mukherjee, Sanjay Puri, and M. Zannetti, arXiv:1006.0934.
- (53) L. Berthier, J.-L. Barrat and J. Kurchan, Eur. Phys. J. B **11**, 635 (1999). F. Corberi, E. Lippiello, and M. Zannetti, Phys. Rev. E **63**, 061506 (2001); Eur. Phys. J. B **24**, 359 (2001).
- (54) Y. C. Chou and W. I. Goldburg, Phys. Rev. A **23**, 858 (1981). S. Katano and M. Iizumi, Phys. Rev. Lett. **52**, 835 (1984). S. Komura, K. Osamura, H. Fujii, and T. Takeda, Phys. Rev. B **31**, 1278 (1985). B. D. Gaulin, S. Spooner, and Y. Mori, Phys. Rev. Lett. **59**, 668 (1987). A. Sicilia, J. J. Arenzon, I. Dierking, A. J. Bray, L. F. Cugliandolo, J. Martínez-Perdiguero, I. Alonso, and I. C. Pintre, Phys. Rev. Lett. **101**, 197801 (2008).
- (55) J. L. Iguain, S. Bustingorry, A. B. Kolton, and L. F. Cugliandolo, Phys. Rev. B **80**, 094201 (2009).
- (56) A. D. Rutenberg and A. J. Bray, Phys. Rev. Lett. **74**, 3836 (1995).
- (57) A. J. Bray and D. K. Jervis, Phys. Rev. Lett. **84**, 1503 (2000).
- (58) N. Andrenacci, F. Corberi, and E. Lippiello, Phys. Rev. E **74** (2006).
- (59) R. Burioni, F. Corberi, and A. Vezzani, Phys. Rev. E **79**, 041119 (2009).
- (60) A. Coniglio and M. Zannetti, Europhys. Lett. **10**, 575 (1989). A. Coniglio, P. Ruggiero, and M. Zannetti, Phys. Rev. E **50**, 1046 (1994).
- (61) S. Bustingorry, J. L. Iguain, and L. F. Cugliandolo, J. Stat. Mech. P09008 (2007). Y. L. Chou and M. Pleimling J. Stat. Mech. P08007 (2010).
- (62) S. Bustingorry, J. Stat. Mech. P10002 (2007).
- (63) A. J. Bray and M. A. Moore, Phys. Rev. Lett. **58**, 57 (1987).

32 References

- (64) D. S. Fisher and D. A. Huse, Phys. Rev. B **38**, 386 (1988)
- (65) D. S. Fisher and D. A. Huse, Phys. Rev. B **43**, 10728 (1991).
- (66) D. S. Fisher, M. P. A. Fisher, and D. A. Huse, Phys. Rev. B **43**, 130 (1991).
- (67) C. Monthus and T. Garel, J. Stat. Mech. P07002 (2008); J. Phys. A **41**, 499801 (2008).
- (68) H. Yoshino (2001), unpublished.
- (69) F. Corberi, A. de Candia, E. Lippiello, and M. Zannetti, Phys. Rev. E **65**, 046114 (2002).
- (70) Y. G. Sinai, Theor. Probab. Appl. **27**, 247 (1982).
- (71) D. S. Fisher, P. Le Doussal, and C. Monthus, Phys. Rev. Lett. **80**, 3539 (1998),
P. Le Doussal, C. Monthus, and D. S. Fisher, Phys. Rev. E **59**, 4975 (1998).
- (72) P. Le Doussal and V. M. Vinokur, Physica C: Superconductivity **254**, 63-68 (1995).
- (73) L. Berthier and J.-P. Bouchaud, Phys. Rev. B **66**, 054404 (2002).
- (74) M. Sales and H. Yoshino, Phys. Rev. E **65**, 066131 (2002).
- (75) M. Sasaki, K. Hukushima, H. Yoshino, and H. Takayama, Phys. Rev. Lett. **95**, 267203 (2005).
- (76) F. Scheffler, H. Yoshino, and P. Maass, Phys. Rev. B **68**, 060404R (2003).
- (77) P. Jonsson, H. Yoshino, and P. Nordblad, Phys. Rev. Lett. **89**, 097201 (2002)
and *ibid* **90**, 059702 (2003).
- (78) H. Yoshino, A. Lemaitre, and J.-P. Bouchaud, Eur. Phys. J B **20**, 367 (2001).
- (79) H. Yoshino and T. Rizzo Phys. Rev. B **77**, 104429 (2008).
- (80) H. Yoshino, J. Phys. A: Math Gen. **36** (2003).
- (81) P. E. Jonsson, R. Mathieu, P. Nordblad, H. Yoshino, H. Aruga Katori, and A. Ito, Phys. Rev. B. **70**, 174402 (2004).
- (82) J-P Bouchaud, L. F. Cugliandolo, J. Kurchan, and M. Mézard, Physica A **226**, 243 (1996).
- (83) A. Parsaeian and H. E. Castillo, Phys. Rev. Lett. **102**, 055704 (2009). Phys. Rev. E **78**, 060105 (2008). H. E. Castillo and A. Parsaeian, Nature Physics **3**, 26 (2007).
- (84) A. Annibale and P. Sollich, J. Stat. Mech. (2009) P02064.
- (85) L. Berthier, Phys. Rev. Lett. **98**, 220601 (2007).
- (86) A. Barrat, Phys. Rev. E **55**, 5651 (1997). H. Yoshino, J. Phys. A **29**, 1421 (1996);
Phys. Rev. Lett. **81**, 1493 (1998). S. Bustingorry, J. L. Iguain, C. Chamon, L. F. Cugliandolo, and D. Domínguez, Europhys. Lett. **76**, 856 (2006).
- (87) L. Berthier, J.-L. Barrat, and J. Kurchan, Phys. Rev. E **63**, 016105 (2001).
- (88) D. A. Huse and C. L. Henley, Phys. Rev. Lett. **54**, 2708 (1985).
- (89) S. Puri, D. Chowdhury, and N. Parekh, J. Phys. A **24**, L1087 (1991). A. J. Bray and K. Humayun, J. Phys. A **24**, L1185 (1991).
- (90) R. Paul, S. Puri, and H. Rieger, Europhys. Lett. **68**, 881 (2004); Phys. Rev. E **71**, 061109 (2005). H. Rieger, G. Schehr, and R. Paul, Prog. Theor. Phys. Suppl. **157**, 111 (2005).
- (91) H. Park and M. Pleimling, arXiv:1009.1677.
- (92) P. Le Doussal, *Exact results and open questions in first principle functional RG*, arXiv:0809.1192.

- (93) G. Schehr and P. Le Doussal, Phys. Rev. E **68**, 046101 (2003); Phys. Rev. Lett. **93**, 217201 (2004). G. Schehr and H. Rieger, Phys. Rev. B **71**, 184202 (2005).
- (94) S. Franz and G. Parisi, J. Phys. C **12**, 6335 (2000).
- (95) G. Biroli and J-P Bouchaud, Europhys. Lett. **67**, 21 (2004).
- (96) G. C. Cianci, R. E. Courtland, and E. R. Weeks, Solid State Comm. **139**, 599 (2006). P. Yunker, Z. X. Zhang, K. B. Aptowicz, and A. G. Yodh Phys. Rev. Lett. **103**, 115701 (2009).
- (97) G. H. Fredrickson and H. C. Andersen, Phys. Rev. Lett. **53**, 1244 (1984); J. Chem. Phys. **83**, 5822 (1985).
- (98) J. Jäckle, J. Phys. Cond.Matt. **14**, 1423 (2002). P. Sollich and F. Ritort, Adv. in Phys. **52**, 219 (2003). S. Leonard, P. Mayer, P. Sollich, L. Berthier, and J. P. Garrahan, J. Stat. Mech. (2007) P07017.
- (99) A. Crisanti, F. Ritort, A. Rocco, and M. Sellitto, J. Chem. Phys. **113**, 10615 (2000). P. Sollich and M. R. Evans, Phys. Rev. Lett. **83**, 3238 (1999). J. P. Garrahan and M. E. J. Newman, Phys. Rev. E **62**, 7670 (2000). S. N. Majumdar, D. S. Dean, and P. Grassberger, Phys. Rev. Lett. **86**, 2301 (2001).
- (100) C. Toninelli and G. Biroli, G. Biroli and C. Toninelli, Eur. Phys. J. B **64** 567 (2008); C. Toninelli and G. Biroli, J. Stat. Phys. **130** 83 (2008).
- (101) F. Corberi and L. F. Cugliandolo, J. Stat. Mech. (2009) P09015.
- (102) See, e.g. R. G. Larson, *The structure and Rheology of Complex fluids* (Oxford University Press, New York, 1999).
- (103) T. Otha, N. Nozaki and M. Doi, Phys. Lett. A **145**, 304 (1990); J. Chem. Phys. **93**, 2664 (1991).
- (104) C. K. Chan, F. Perrot, and D. Beysens, Phys. Rev. A **43**, 1826 (1991). T. Takebe, F. Fujioka, R. Sawaoka, and T. Hashimoto, J. Chem. Phys. **98**, 717 (1993). T. Hashimoto, K. Matsuzaka, E. Moses, and A. Onuki, Phys. Rev. Lett. **74**, 126 (1995). J. Läger, C. Laubner, and W. Gronsky, Phys. Rev. Lett. **75**, 3576 (1995). R. Yamamoto and X. C. Zeng, Phys. Rev. E **59**, 3223 (1997). Z. Shou and A. Chakrabarti, Phys. Rev. E **61**, R2200 (2000). H. Liu and A. Chakrabarti, J. Chem. Phys. **112**, 10582 (2000).
- (105) F. Corberi, G. Gonnella, and A. Lamura, Phys. Rev. Lett. **81**, 3852 (1998); Phys. Rev. E **61**, 6621 (2000). N. P. Rapapa and A. J. Bray, Phys. Rev. Lett. **83**, 3856 (1999).
- (106) A. J. Bray and A. Cavagna, J. Phys. A **33**, L305 (2000). A. J. Bray, A. Cavagna, and Rui D. M. Travasso, Phys. Rev. E **64**, 012102 (2001); Phys. Rev. E **65**, 016104 (2002).
- (107) P. Padilla and S. Toxvaerd, J. Chem. Phys. **106**, 2342 (1997). M. E. Cates, V. M. Kendon, P. Bladon, and J.-C. Despat, Faraday Discuss. **112**, 1 (1999). F. Corberi, G. Gonnella, and A. Lamura, Phys. Rev. Lett. **83**, 4057 (1999); Phys. Rev. E **62**, 8064 (2000).
- (108) P. Stansell, K. Stratford, J.-C. Despat, R. Adhikari and M. E. Cates, Phys. Rev. Lett. **96**, 085701 (2006).
- (109) F. Corberi, G. Gonnella, E. Lippiello and M. Zannetti, Europhys. Lett. **60**, 425 (2002); J. Phys. A **36**, 4729 (2003).

34 References

- (110) L. F. Cugliandolo, J. Kurchan, P. Le Doussal, and L. Peliti, Phys. Rev. Lett. **78**, 350 (1997).
- (111) J-L Barrat and L. Berthier, Phys. Rev. Lett. **89**, 095702 (2002). J. Chem. Phys. **116**, 6228 (2002).
- (112) D. Bonn, S. Tanase, B. Abou, H. Tanaka, and J. Meunier, Phys. Rev. Lett. **89**, 015701 (2002). B. Viasnoff and F. Lequeux, Phys. Rev. Lett. **89**, 065701 (2002).
- (113) G. Petekis, A. Moussald, and P. N. Pusey, Phys. Rev. E **66**, 051402 (2002).
- (114) R. Di Leonardo, F. Ianni, and G. Ruocco, Phys. Rev. E **71**, 011505 (2005).
- (115) D. Chen, D. Semwogerere, J. Sato, V. Breedveld, and E. R. Weeks, arXiv:0908.4226.
- (116) J. Rottler and M. Warren, Eur. Phys. J. Sp. Topics **161**, 55 (2008).
- (117) J-L Barrat, J. Baschnagel, and A. Lyulin, arXiv:1002.2065.
- (118) G. Schehr and P. Le Doussal, Europhys. Lett. **71**, 290 (2005). A. B. Kolton, A. Rosso, E. V. Albano, and T. Giamarchi, Phys. Rev. B **74**, 140201(R) (2006). A. B. Kolton, G. Schehr, and P. Le Doussal, Phys. Rev. Lett. **103**, 160602 (2009).
- (119) O. Dauchot, *Glassy behaviours in a-thermal systems, the case of granular media: A tentative review*, Lecture Notes in Physics **716**, 161 (2007).
- (120) A. Kabla and G. Debregeas, Phys. Rev. Lett. **92**, 035501 (2004).
- (121) O. Dauchot, G. Marty, and G. Biroli, Phys. Rev. Lett. **95**, 265701 (2005). F. Lechenault, O. Dauchot, G. Biroli, and J-P Bouchaud, EPL **83**, 46002 (2008).
- (122) L. Berthier, L. F. Cugliandolo, and J. L. Iguain, Phys. Rev. E **63**, 051302 (2001).
- (123) C. Aron, G. Biroli, and L. F. Cugliandolo, Phys. Rev. Lett. **102**, 050404 (2009). S. Franz, G. Parisi, F. Ricci-Tersenghi, and T. Rizzo, arXiv:1008.0996.
- (124) H. Sompolinsky, Phys. Rev. Lett. **47**, 935 (1981).
- (125) S. L. Ginzburg, Zh. Eksp. Teor. Fiz. **90**, 754 (1986) [Sov. Phys. JETP **63**, 439 (1986)]. L. B. Ioffe, Phys. Rev. B **38**, 5181 (1988).
- (126) A. Montanari and G. Semerjian, J. Stat. Phys. **125**, 23 (2006).